RECORD #
4AA0007
AAB3185

SECURITY INFORMATION

CONFIDENTIAL

CLASSIFICATION cancelled
JUL 20 1956

Copy 77
RM L53A09a

NACA RM L53A09a

AERONAUTICS LIBRARY
California Institute of Technology

NACA

RESEARCH MEMORANDUM

INVESTIGATION OF THE EFFECTS OF LEADING-EDGE CHORD-EXTENSIONS AND FENCES IN COMBINATION WITH LEADING-EDGE FLAPS ON THE AERODYNAMIC CHARACTERISTICS AT MACH NUMBERS FROM 0.40 TO 0.93 OF A 45° SWEPTBACK WING OF ASPECT RATIO 4

By Kenneth P. Spreemann and William J. Alford, Jr.

Langley Aeronautical Laboratory
Langley Field, Va.

CLASSIFIED DOCUMENT

This material contains information affecting the National Defense of the United States within the meaning of the espionage laws, Title 18, U.S.C., Secs. 793 and 794, the transmission or revelation of which in any manner to an unauthorized person is prohibited by law.

NATIONAL ADVISORY COMMITTEE FOR AERONAUTICS

WASHINGTON

February 19, 1953

CLASSIFICATION cancelled

CONFIDENTIAL

NATIONAL ADVISORY COMMITTEE FOR AERONAUTICS

RESEARCH MEMORANDUM

INVESTIGATION OF THE EFFECTS OF LEADING-EDGE CHORD-EXTENSIONS AND FENCES IN COMBINATION WITH LEADING-EDGE FLAPS ON THE AERODYNAMIC CHARACTERISTICS AT MACH NUMBERS FROM 0.40 TO 0.93 OF A 45° SWEPTBACK WING OF ASPECT RATIO 4

By Kenneth P. Spreemann and William J. Alford, Jr.

SUMMARY

This investigation was made to determine the effects of 6° full-span and 3° partial-span leading-edge flaps in combination with chord-extensions or fences on the aerodynamic characteristics of a wing-fuselage configuration with a 45° sweptback wing of aspect ratio 4, taper ratio 0.3, and NACA 65A006 airfoil sections. The investigation was made in the Langley high-speed 7- by 10-foot tunnel over a Mach number range of 0.40 to 0.93 and an angle-of-attack range of about -2° to 24°. Lift, drag, and pitching-moment data were obtained for all configurations.

All the chord-extensions or fences in combination with the 6° full-span and 3° partial-span leading-edge flaps delayed the unstable pitching tendencies to much higher lift coefficients than those obtainable with the basic wing up to Mach numbers of 0.80 to 0.85. Beginning at a Mach number of about 0.80 to 0.85 the improvements in the pitching moments in the high lift range were considerably reduced for all the modifications investigated. The leading-edge flap configurations alone or the chord-extension alone (no leading-edge flap deflection) were less effective than the combination of the two devices in delaying the unstable pitching-moment tendencies to higher lift coefficients.

All modifications generally increased the maximum lift-drag ratios about 10 to 20 percent up to a Mach number of about 0.90. The minimum drag coefficients and the lift coefficients for maximum lift-drag ratios were increased by all of the modifications; however the 3° partial-span leading-edge flap configurations gave about half the increases provided by the 6° full-span leading-edge flap configurations.

From over-all considerations of stability and performance it appears that with the model of this investigation the 6° full-span leading-edge flaps in combination with the chord-extension over the outboard 35 percent of the span, with or without leading-edge camber, would be the most desirable configuration.

INTRODUCTION

In order to obtain the full benefits of the high lift coefficients obtainable with a thin sweptback wing, the detrimental effects of high drag and instability in the high lift range must be overcome. Flow surveys have shown that tip separation on a thin sweptback wing is strongly influenced by a leading-edge separation vortex that is generated on the upper surface. (For a more detailed discussion of this type of flow phenomenon, see refs. 1 and 2.) Low-speed wind-tunnel tests (refs. 2 and 3) have shown that the high lift stability characteristics can be improved by causing the leading-edge separation vortex to shed from the wing before growing large enough to cause tip separation. This controlled shedding of the leading-edge vortex can be effected by use of an obstruction such as a fence or by a chordwise discontinuity such as a leading-edge chord-extension, which seems to provide an aerodynamic barrier to the growth of the leading-edge vortex.

In a previous investigation (ref. 4), outboard leading-edge chord-extensions or fences, when employed on the present wing-fuselage combination, provided substantial improvements in high-lift longitudinal stability characteristics, at least within the Mach number range below 0.90. Such devices, however, had only small effects on performance characteristics. Other investigations (for example, refs. 5 and 6) have shown that by deflecting a leading-edge flap appreciable increases in lift-drag ratios can be achieved at Mach numbers up to 0.90 but with little improvement in high-lift stability. Therefore, the purpose of the present investigation was to determine to what extent the gains realized through the use of chord-extensions or fences to improve high-lift stability and the use of leading-edge flaps to improve lift-drag ratios could be combined to improve simultaneously the high-lift stability and the lift-drag ratios.

Unpublished results of full-span and partial-span leading-edge flaps of 3°, 6°, 10°, and 15° deflection on the wing used in the present investigation indicated that the 6° full-span and 3° partial-span flaps were, in general, the best leading-edge flap arrangements for improving the lift-drag ratios of this model; consequently these two flap configurations were selected for the present investigation. This investigation was made to determine the effects of these two flap arrangments in combination with chord-extensions or fences on the aerodynamic characteristics of a wing-fuselage configuration with a 45° sweptback wing of aspect ratio 4, taper ratio 0.3, and NACA 65A006 airfoil sections.

The investigation was made in the Langley high-speed 7- by 10-foot tunnel over a Mach number range of 0.40 to 0.93 and an angle-of-attack range of about -2° to 24°. Lift, drag, and pitching moments were obtained for all configurations.

COEFFICIENTS AND SYMBOLS

All coefficients presented herein are based on the wing area without chord-extensions. The coefficients and symbols used in this paper are defined as follows:

C_L	lift coefficient, $\frac{\text{Lift}}{qS_w}$
C_D	drag coefficient, $\frac{\text{Drag}}{qS_w}$
C_m	pitching-moment coefficient referred to $0.25\bar{c}$, $\frac{\text{Pitching moment}}{qS_w\bar{c}}$
q	dynamic pressure, $\frac{1}{2}\rho V^2$, lb/sq ft
S_w	wing area, sq ft
S_b	area of base of model, sq ft
$\bar{c}$	mean aerodynamic chord of wing, $\frac{2}{S}\int_0^{b/2} c^2 dy$, ft
c	local wing chord, parallel to plane of symmetry, ft
b	wing span, ft
ρ	air density, slugs/cu ft
V	free-stream velocity, ft/sec
P_o	free-stream static pressure, lb/sq ft
M	Mach number
R	Reynolds number of wing based on $\bar{c}$
α	angle of attack of fuselage center line, deg
$\Delta\alpha$	local angle-of-attack change due to distortion of wing, deg
K	correction factor for C_{L_α} due to wing distortion

C_{L_α} lift-curve slope, $\frac{\partial C_L}{\partial \alpha}$

$\Delta\left(\frac{\partial C_m}{\partial \alpha}\right)$ incremental change in aerodynamic-center location due to wing distortion

y spanwise distance from plane of symmetry, ft

δ_{n_A} flap deflection of inboard leading-edge flaps (0.139b/2 to 0.426b/2 shown in fig. 1), deg

δ_{n_B} flap deflection of outboard leading-edge flaps (0.426b/2 to 1.00b/2 shown in fig. 1), deg

C_{m_o} pitching-moment coefficient at zero lift coefficient

$C_{D_{min}}$ minimum drag coefficient

$(L/D)_{max}$ maximum lift-drag ratio

$\frac{(L/D)_{mod}}{(L/D)_{basic}}$ performance ratio; lift-drag ratio of modified wing-fuselage configurations referred to the lift-drag ratio of basic wing-fuselage configuration

$C_{L_{(L/D)_{max}}}$ lift coefficient at maximum lift-drag ratio

MODEL AND APPARATUS

A drawing of the wing-fuselage combination showing details of the leading-edge flaps and chord-extensions employed is presented in figure 1. Details of the fence and fence positions tested are shown in figure 2. A photograph of the model, with 6° full-span flap and a chord-extension, mounted on the sting in the Langley high-speed 7- by 10-foot tunnel, is shown in figure 3. The wing employed in this investigation had 45° sweepback of the quarter-chord line, aspect ratio 4, taper ratio 0.3, and an NACA 65A006 airfoil section parallel to the plane of symmetry. Ordinates of the fuselage are given in table I.

The 6° full-span flap (designated as $\delta_{n_A} = 6°$, $\delta_{n_B} = 6°$) was investigated in combination with the chordwise extensions of 10 percent $\bar{c}$ from 0.65b/2 to the tip and from 0.70b/2 to the tip. Tests of the chord-extension from 0.65b/2 to tip also were made with the leading edge of the chord-extension modified to provide camber and a further addition of 1.0 percent of the local wing chord to the chord-extension. Two fence

configurations were also investigated in combination with the 6° full-span flap; one fence was at 0.65b/2 and the other was at 0.50b/2. The fences were 105 percent of the streamwise chords in length and were made of 1/16-inch-thick duralumin.

The 3° partial-span flap (outboard 0.426b/2 to tip deflected to 3° and designated as $\delta_{n_A} = 0^{\circ}$, $\delta_{n_B} = 3^{\circ}$) was investigated in combination with a chordwise extension of 10 percent $\bar{c}$ from 0.65b/2 to the tip. The modified leading-edge chord-extension with a cambered leading edge and a further addition of 1.0 percent of the local wing chord to the chord-extension was also tested on this configuration.

The flap was established by cutting the wing along the 20-percent-chord line, and flap angles were obtained with preset steel inserts. After setting a desired flap angle, the groove in the wing was filled and finished off flush to the wing surface. The chord-extension was made by using a larger insert to extend the nose section forward $0.10\bar{c}$. The two segments of the airfoil (nose and trailing-edge sections) were joined by a smooth fairing. (See figs. 1 and 3). Angular distortion of the flap and chord-extension under load was negligible.

The model was tested on the sting-type support system shown in figure 3. With this system the model was remotely operated through an angle-of-attack range of about -2° to 24°. A strain-gage balance mounted inside the fuselage was used to measure the forces and moments of the wing-fuselage combination.

TESTS AND CORRECTIONS

The investigation was made in the Langley high-speed 7- by 10-foot tunnel. Lift, drag, and pitching moment were measured through a Mach number range of 0.40 to 0.93 and an angle-of-attack range of about -2° to 24°. The size of the model caused the tunnel to choke at a corrected Mach number of about 0.95 for the zero-lift condition, although partial-choking conditions may have occurred in the high angle-of-attack range at a Mach number of the order of 0.93.

Blockage corrections were determined by the method of reference 7 and were applied to the Mach numbers and dynamic pressures. Jet-boundary corrections, applied to the angle of attack and drag, were calculated by the method of reference 8. The jet-boundary corrections to pitching moment were considered negligible and were not applied to the data. Corrections for vertical buoyancy on the support strut and for longitudinal pressure gradient were also considered negligible and were not applied to the data.

No tare corrections were obtained; however, previous experience (ref. 9, for example) indicates that for a tailless sting-mounted model, similar to the model investigated herein, the tare corrections to lift and pitching moment are negligible. The drag data have been corrected to correspond to a pressure at the base of the fuselage equal to free-stream static pressure. For this correction, the base pressure was determined by measuring the pressure inside the fuselage at a point about 9 inches forward of the base. The drag correction (base pressure drag coefficient C_{D_b}) was calculated from the measured pressure data by the relation

$$C_{D_b} = \frac{P_b - P_o}{q} \frac{S_b}{S_w}$$

Values of C_{D_b} for average test conditions are presented in figure 4. The corrected model drag data were obtained by adding the base pressure drag coefficient to the drag coefficient determined from the strain-gage measurements.

The angle of attack has been corrected for deflection of the sting-support system under load. Correction factors for the effects of aero-elastic distortion of the wing were obtained by static loading to simulate elliptic span loading and these correction factors are presented in figure 5. These correction factors were not applied to the data.

The mean Reynolds number variation with Mach number for the wing of this investigation is presented in figure 6.

RESULTS AND DISCUSSION

The data are presented in figures 7 to 18; a detailed listing of the data is given in table II. The data for the basic wing are presented in each figure for a basis of comparison and data for each configuration are given for a range of Mach numbers from 0.40 to 0.93. The slopes presented in figures 15 to 18 have been averaged over a lift-coefficient range of about 0 to 0.4.

Lift Characteristics

Some aspects of the lift in this paper are pertinent to the purpose of obtaining lower drag at high lift; consequently the lift characteristics are in general discussed in this vein. The 6° full-span leading-edge flaps with plain chord-extensions (configurations 3 and 4) gave

larger gains in lift over the basic wing-fuselage configuration (configuration 1) in the high angle-of-attack range than those obtained with the 6° full-span flap alone (configuration 2) particularly below 0.80 Mach number (fig. 7(a)). However it may be observed that in the high Mach number range (0.80 to 0.90) the leading-edge flap alone gave about the same gains in lift as when in combination with the chord-extension. Included in figure 8 are the aerodynamic characteristics of a chord-extension running from 0.65b/2 to the tip without leading-edge flaps (from ref. 4). These results are presented in this paper to give a more complete evaluation of leading-edge flap and chord-extension combinations. It can be observed in figure 8(a) that the chord-extension alone (configuration 5) was not as effective as when combined with the leading-edge flap (configuration 3) in extending the lift coefficient in the high angle-of-attack range below a Mach number of 0.85. Comparison of figures 7(a) and 10(a) shows that the addition of either fence configuration to the 6° full-span flap (configurations 10 and 11) did not greatly alter the increases in lift coefficient in the high angle-of-attack range from those of the 6° full-span flap alone (configuration 2). The 3° partial-span leading-edge flaps and chord-extension combinations (fig. 9(a), configurations 8 and 9) generally gave no more than half the increases in lift coefficient in the high angle-of-attack range that were given with the 6° full-span leading-edge flap with chord-extensions (fig. 7(a), configurations 3 and 4).

The lift-curve slopes $\frac{\partial C_L}{\partial \alpha}$ would not be expected to be greatly affected by any of the modifications of this investigation, and as can be observed in figures 15 to 18 the increases in $\frac{\partial C_L}{\partial \alpha}$ over the basic wing were no more than about 4 to 6 percent. Note that point values are given in the summary figure for the 0.50b/2 fence because it was felt that insufficient data were obtained to warrant faired curves.

The 6° full-span flaps and modifications thereto usually gave positive angles of attack for zero lift, $\alpha_{C_{L=0}}$, throughout the test range of Mach number; whereas the 3° partial-span flaps and modifications provided negative values of $\alpha_{C_{L=0}}$ above a Mach number of about 0.65 (figs. 15 to 18). A similar reversal in $\alpha_{C_{L=0}}$ was obtained for a 3.3° partial-span leading-edge flap reported in reference 5. This unusual result may be attributable to induced effects in the vicinity of the flap juncture with the chord-extension.

Drag Characteristics

All modifications involving the 6° full-span leading-edge flaps (configurations 2, 3, 4, and 6) including the two fence configurations (configurations 10 and 11) increased the minimum drag coefficient $C_{D_{min}}$ about 0.003 over that of the basic wing up to a Mach number of 0.90. At the highest test Mach number (M = 0.93) $C_{D_{min}}$ for these configurations was increased about 0.006 (figs. 15, 16, and 18). The chord-extension alone (no leading-edge-flap deflection) caused practically no increase in $C_{D_{min}}$ at low Mach numbers but above a Mach number of 0.70 caused an increase in $C_{D_{min}}$ of about half as much as with the flap deflected 6° (fig. 16, configurations 5 and 3). The 3° partial-span leading-edge flaps alone (fig. 17, configuration 7) gave hardly any increase in $C_{D_{min}}$ throughout the Mach number range; however, in combination with the chord-extension and chord-extension plus leading-edge camber (fig. 17, configurations 8 and 9) the 3° partial-span flaps gave about half or two-thirds the increases in $C_{D_{min}}$ indicated with the 6° full-span flaps and modifications.

All modifications involving both the 6° full-span and 3° partial-span leading-edge flaps caused the drag curves to be shifted so that in the high-lift range the drag coefficient for a given lift coefficient was reduced with relation to the basic wing. (See parts (b) of figs. 7 to 10.) It may be noticed in particular that the chord-extensions and chord-extensions plus leading-edge camber (configurations 3, 4, and 6) gave greater reductions in drag relative to the basic wing in the high lift-coefficient range than the other configurations investigated. However, it should be observed that the reductions of C_D in the high-lift range were much less for the 3° partial-span flap configurations than for the 6° full-span flap configurations. From figure 8(b) it can be seen that the chord-extension alone (configuration 5) reduced the drag only in the highest lift range. Furthermore, these reductions were considerably less than those obtained when the chord-extension was employed in combination with either the 6° full-span or 3° partial-span leading-edge flaps. The two fence configurations did not appreciably alter the high-lift drag of the 6° full-span flaps (fig. 7(b), configuration 2 and fig. 10(b), configurations 10 and 11). Considering the nature of these results it appears that the leading-edge flap deflection was the largest single factor in reducing the drag coefficient at the higher lift coefficients.

Lift-Drag Ratios

The 6° full-span leading-edge flap with chord-extensions (configurations 3 and 4, fig. 11) or with chord-extensions plus leading-edge camber (configuration 6, fig. 12) provided substantial improvements in lift-drag

ratios above $C_L = 0.2$ to 0.3 up to a Mach number of about 0.90 over the basic wing-fuselage configuration. The 6° full-span flap alone (configuration 2) gave somewhat smaller improvements. In figures 15 and 16 it may be observed that at $C_L = 0.70$ the lift-drag ratios for the 6° full-span flaps and chord-extensions (configurations 3, 4, and 6) were about 30 to 60 percent higher than those of the basic wing-fuselage configuration. Above a Mach number of about 0.75 the 6° full-span flaps alone (configuration 2) gave about the same improvements as with chord-extensions. All 6° full-span flaps and chord-extensions lost most of their effectiveness in the limited Mach number range between 0.90 to 0.93. From figures 12 and 16 it is apparent that the chord-extensions with no leading-edge flaps (configuration 5) gave much smaller improvements in lift-drag ratios in any lift or Mach number range than with leading-edge flaps, for example, at $C_L = 0.70$ about 4- to 6-percent improvement compared to 30- to 60-percent improvement with leading-edge flaps. The 3° partial-span flap configurations afforded about half the increases in lift-drag ratios that were obtained with the 6° full-span flap configurations. (See figs. 13 and 17.) The fence configurations in combination with the 6° full-span flaps (configurations 10 and 11, fig. 14) did not greatly affect the improvements in lift-drag ratios realized by the 6° full-span leading-edge flaps alone (configuration 2, fig. 11).

The maximum lift-drag ratios of the configurations with leading-edge flaps, chord-extensions, and fences have been referred to the maximum lift-drag ratios of the basic wing-fuselage configuration to give the performance parameter $\frac{(L/D)_{max_{mod}}}{(L/D)_{max_{basic}}}$ (see figs. 15 to 18). Models tested in various test facilities such as the transonic bump, reflection plane, and sting have shown differences in values of $C_{D_{min}}$ and $(L/D)_{max}$ for tests of the same model configuration (ref. 10); consequently it is believed that this performance ratio is a more reliable basis for comparison than the actual values of $(L/D)_{max}$.

The parameter $\frac{(L/D)_{max_{mod}}}{(L/D)_{max_{basic}}}$ indicates that chord-extensions on the 6° full-span flap (configurations 3 and 4, fig. 15) increased $(L/D)_{max}$ about 10 to 15 percent over that of the basic wing-fuselage configuration up to a Mach number of about 0.90, but the 6° full-span leading-edge flap alone (configuration 2) gave only about half the increase in $(L/D)_{max}$ afforded when in combination with the chord-extension. Addition of the cambered leading edge to the chord extension from $0.65b/2$ to tip (configuration 6, fig. 16) increased the improvements in $(L/D)_{max}$ to about 15 to 20 percent. From figure 16 it can also be seen that the chord-extension alone (no leading-edge flap deflection, configuration 5) gave

values of $(L/D)_{max}$ somewhat lower than those of the basic wing-fuselage combination. The 3° partial-span flap and chord-extension modifications produced somewhat smaller improvements in $(L/D)_{max}$ than the 6° full-span flap modifications (figs. 15, 16, and 17). The two fence configurations had little or no effect on $(L/D)_{max}$, which as shown in figure 18 gave about the same values of $(L/D)_{max}$ as the 6° full-span flap alone. All modifications to the wing leading edge lost effectiveness above a Mach number of 0.90 except the 3° partial-span flap alone (configuration 7, fig. 17), which maintained values of $(L/D)_{max}$ greater or equal to those of the basic wing-fuselage combination throughout the Mach number range investigated. The effectiveness of the 3° partial-span flap alone on $(L/D)_{max}$ at the highest Mach number probably can be attributed largely to the low values of $C_{D_{min}}$ for this particular configuration.

All 6° full-span flap modifications increased the lift coefficient at maximum lift-drag ratio $C_{L_{(L/D)_{max}}}$ about 0.05 to 0.10 over that of the basic wing-fuselage configuration. The 3° partial-span flap modifications gave about half the increases in $C_{L_{(L/D)_{max}}}$ given by the 6° full-span flap modifications.

Pitching-Moment Characteristics

With either the 6° full-span or the 3° partial-span leading-edge flaps, all chord-extensions, chord-extensions plus cambered leading edge, and fences provided improved stability characteristics over those of the basic wing-fuselage combination at the higher lift coefficients and angles of attack. (See parts (c) and (d) of figs. 7 to 10.) Both flap deflections alone (configurations 2 and 7, parts (c) and (d) of figs. 7 and 9) delayed the unstable tendencies to higher lift coefficients and angles of attack but not nearly as much as when in combination with the aforementioned modifications. The chord-extensions alone (configuration 5, fig. 8) delayed the departures from linearity to higher lift coefficients and angles of attack but as may be observed from parts (c) and (d) of figures 8 and 9 they were not quite as effective as when in combination with the 6° full-span or 3° partial-span flaps.

The 6° full-span and 3° partial-span flaps alone (configurations 2 and 7, parts (c) and (d) of figs. 7 and 9) delayed the instability about 0.10 C_L and about 1° to 2° beyond that of the basic wing-fuselage configuration; whereas when in combination with the plain chord-extension or chord-extension plus leading-edge camber (configurations 3, 4, 6, 8, and 9, parts (c) and (d) of figs. 7, 8, and 9) these values were usually more than doubled. However, above a Mach number of about 0.85 the improvements diminished for all the leading-edge modifications employed. The

chord-extension plus leading-edge camber on either the 6° full-span or the 3° partial-span flaps (configurations 6 and 9) retained slightly more effectiveness than any other modifications at the highest Mach numbers investigated; at a Mach number of 0.93 the pitch-up was delayed about 0.3 C_L or about 4° angle of attack relative to the basic wing-fuselage configuration (see parts (c) and (d) of figs. 8 and 9). However, because the tunnel may have been near choking conditions above an angle of attack of 7° or 8° at a Mach number of 0.93, points above these angles may be of questionable value. The improved stability which occurs throughout the Mach number range seems to result from improved flow over the outboard wing section with chord-extensions installed, as is reflected by increases in lift and reductions in drag at the higher angles of attack.

The two fence configurations in combination with the 6° full-span leading-edge flaps were somewhat less effective than the chord-extensions in delaying instability to higher lift coefficients and angles of attack (parts (c) and (d) of fig. 10). In general all the chord-extensions and fences employed delayed the instability to considerably higher lift coefficients and angles of attack, although the departures from linearity in the high lift and angle-of-attack range still may be undesirable on the basis of dynamic-stability considerations. From over-all considerations of stability and performance it appears that with the model of this investigation the 6° full-span leading-edge flaps in combination with the chord-extension over the outboard 35 percent of the span, with or without leading-edge camber, would be the most desirable configuration.

Curves of the pitching-moment slopes $\frac{\partial C_m}{\partial C_L}$ in the low-lift range show that Mach number effects on the aerodynamic-center location were not greatly altered by any of the modifications to the basic wing-fuselage configuration employed (figs. 15 to 18). All the modifications usually showed a tendency to shift the aerodynamic-center location slightly forward below Mach numbers of 0.80 to 0.85 and to provide a slight rearward shift above these Mach numbers.

The pitching-moment coefficients for zero lift C_{m_0} (figs. 15 to 18) were not greatly affected by any modification employed, except for a general tendency to become somewhat more negative with Mach number; thus trim changes attributable to the wing-fuselage configuration that may be affected by any of these modifications would be rather small.

CONCLUSIONS

An investigation of the effects of a number of leading-edge modifications and fences on the aerodynamic characteristics of a 45° sweptback wing of aspect ratio 4 indicate the following conclusions:

1. All the chord-extensions, chord-extensions plus leading-edge camber, and fences in combination with the 6° full-span and 3° partial-span leading-edge flaps delayed instability to much higher lift coefficients than those obtainable with the basic wing up to Mach numbers of 0.80 to 0.85. Beginning at a Mach number of about 0.80 to 0.85 the improvements in the pitching moment in the high lift range were considerably reduced for all the modifications investigated.

2. The leading-edge flap alone and the chord-extension alone (no leading-edge flap) were less effective than when combined in delaying the unstable pitching-moment tendencies to higher lift coefficients.

3. All modifications incorporating leading-edge flaps generally increased the maximum lift-drag ratios about 10 to 20 percent up to a Mach number of about 0.90. Above a Mach number of 0.90 all of the modifications lost effectiveness except the 3° partial-span flap alone, which gave increases in the maximum lift-drag ratios up to a Mach number of 0.93.

4. The 6° full-span leading-edge flap and modifications increased the lift-drag ratios at a lift coefficient of 0.70 about 30 to 60 percent over those of the basic wing-fuselage configuration throughout the Mach number range investigated; whereas the 3° partial-span leading-edge flaps and modifications gave about half these increases at a lift coefficient of 0.70.

5. The minimum drag coefficients and the lift coefficient for maximum lift-drag ratios were increased by all modifications; however the 3° partial-span leading-edge flap configurations gave about half the increases provided by the 6° full-span leading-edge flap configurations.

6. In general all modifications showed no significant effects on the lift-curve slopes, angle of attack for zero lift, aerodynamic-center location, and pitching moment for zero lift.

7. From over-all considerations of stability and performance it appears that with the model of this investigation the 6° full-span leading-edge flaps in combination with the chord-extension over the outboard 35 percent of the span, with or without leading-edge camber, would be the most desirable configuration.

Langley Aeronautical Laboratory,
National Advisory Committee for Aeronautics,
Langley Field, Va.

REFERENCES

1. Furlong, G. Chester, and McHugh, James G.: A Summary and Analysis of the Low-Speed Longitudinal Characteristics of Swept Wings at High Reynolds Number. NACA RM L52D16, 1952.

2. Jaquet, Byron M.: Effects of Chord Discontinuities and Chordwise Fences on Low-Speed Static Longitudinal Stability of an Airplane Model Having 35° Sweptback Wing. NACA RM L52C25, 1952.

3. Goodson, Kenneth W., and Few, Albert G., Jr.: Low-Speed Static Longitudinal and Lateral Stability Characteristics of a Model With Leading-Edge Chord-Extensions Incorporated on a 40° Sweptback Circular-Arc Wing of Aspect Ratio 4 and Taper Ratio 0.50. NACA RM L52I18, 1952.

4. Goodson, Kenneth W., and Few, Albert G., Jr.: Effect of Leading-Edge Chord-Extensions on Subsonic and Transonic Aerodynamic Characteristics of Three Models Having 45° Sweptback Wings of Aspect Ratio 4. NACA RM L52K21, 1953.

5. Spreemann, Kenneth P., and Alford, William J., Jr.: Small-Scale Transonic Investigation of the Effects of Full-Span and Partial-Span Leading-Edge Flaps on the Aerodynamic Characteristics of a 50° 38' Sweptback Wing of Aspect Ratio 2.98. NACA RM L52E12, 1952.

6. Alford, William J., Jr., and Spreemann, Kenneth P.: Small-Scale Transonic Investigation of a 45° Sweptback Wing of Aspect Ratio 4 With Combinations of Nose-Flap Deflections and Wing Twist. NACA RM L52K13, 1953.

7. Herriot, John G.: Blockage Corrections for Three-Dimensional-Flow Closed-Throat Wind Tunnels, With Consideration of the Effect of Compressibility. NACA Rep. 995, 1950. (Supersedes NACA RM A7B28.)

8. Gillis, Clarence L., Polhamus, Edward C., and Gray, Joseph L., Jr.: Charts for Determining Jet-Boundary Corrections for Complete Models in 7- by 10-Foot Closed Rectangular Wind Tunnels. NACA WR L-123, 1945. (Formerly NACA ARR L5G31.)

9. Osborne, Robert S.: High-Speed Wind-Tunnel Investigation of the Longitudinal Stability and Control Characteristics of a $\frac{1}{16}$- Scale Model of the D-558-2 Research Airplane at High Subsonic Mach Numbers and at a Mach Number of 1.2. NACA RM L9C04, 1949.

10. Donlan, Charles J., Myers, Boyd C., II, and Mattson, Axel T.: A Comparison of the Aerodynamic Characteristics at Transonic Speeds of Four Wing-Fuselage Configurations as Determined From Different Test Techniques. NACA RM L50H02, 1950.

TABLE I.- FUSELAGE ORDINATES

[Basic fineness ratio, 12; actual fineness ratio 9.8 achieved by cutting off rear portion of body]

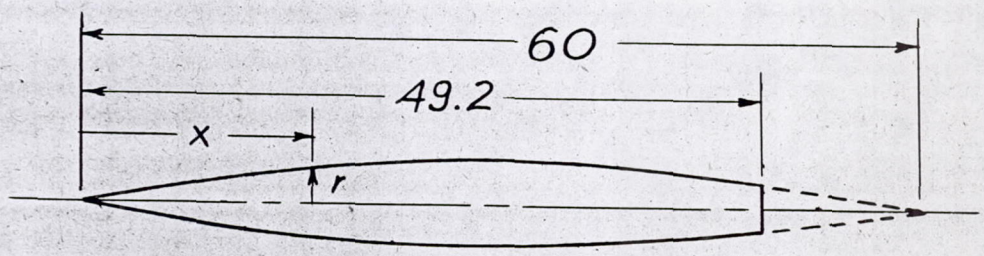

Ordinate, in.	
x	r
0	0
.30	.139
.45	.179
.75	.257
1.50	.433
3.00	.723
4.50	.968
6.00	1.183
9.00	1.556
12.00	1.854
15.00	2.079
18.00	2.245
21.00	2.360
24.00	2.438
27.00	2.486
30.00	2.500
33.00	2.478
36.00	2.414
39.00	2.305
42.00	2.137
49.20	1.650
L.E. radius = 0.030 in.	

TABLE II.- LIST OF FIGURES PRESENTING DATA

Figure	Configuration	δ_{n_A}, deg	δ_{n_B}, deg	Chord-extension	Camber	Fence location	Data presented
7	1 2 3 4	0 6 ↓ ↓	0 6 ↓ ↓	None None 0.65b/2 to tip .70b/2 to tip	None ↓ ↓ ↓	None ↓ ↓ ↓	Basic ↓ ↓ ↓
8	1 5 3 6	0 0 6 6	0 0 6 6	None .65b/2 to tip ↓ ↓	None ↓ On ↓	None ↓ ↓ ↓	Basic ↓ ↓ ↓
9	1 7 8 9	0 ↓ ↓ ↓	0 3 ↓ ↓	None None .65b/2 to tip .65b/2 to tip	None ↓ ↓ On	None ↓ ↓ ↓	Basic ↓ ↓ ↓
10	1 10 11	0 6 6	0 6 6	None ↓ ↓	None ↓ ↓ ↓	None 0.65b/2 .50b/2	Basic ↓ ↓ ↓
11	1 2 3 4	0 6 ↓ ↓	0 6 ↓ ↓	None None .65b/2 to tip .70b/2 to tip	None ↓ ↓ ↓	None ↓ ↓ ↓	L/D ↓ ↓ ↓
12	1 5 3 6	0 0 6 6	0 0 6 6	None .65b/2 to tip ↓ ↓	None ↓ ↓ On	None ↓ ↓ ↓	L/D ↓ ↓ ↓
13	1 7 8 9	0 ↓ ↓ ↓	0 3 ↓ ↓	None None .65b/2 to tip .65b/2 to tip	None ↓ ↓ On	None ↓ ↓ ↓	L/D ↓ ↓ ↓
14	1 10 11	0 6 6	0 6 6	None ↓ ↓	None ↓ ↓ ↓	None .65b/2 .50b/2	L/D ↓ ↓ ↓
15	1 2 3 4	0 6 ↓ ↓	0 6 ↓ ↓	None None .65b/2 to tip .70b/2 to tip	None ↓ ↓ ↓	None ↓ ↓ ↓	Summary ↓ ↓ ↓
16	1 5 3 6	0 0 6 6	0 0 6 6	None .65b/2 to tip ↓ ↓	None ↓ ↓ ↓	None ↓ ↓ ↓	Summary ↓ ↓ ↓
17	1 7 8 9	0 ↓ ↓ ↓	0 3 ↓ ↓	None None .65b/2 to tip .65b/2 to tip	None ↓ ↓ On	None ↓ ↓ ↓	Summary ↓ ↓ ↓
18	1 10 11	0 6 6	0 6 6	None ↓ ↓	None ↓ ↓ ↓	None .65b/2 .50b/2	Summary ↓ ↓ ↓

NACA

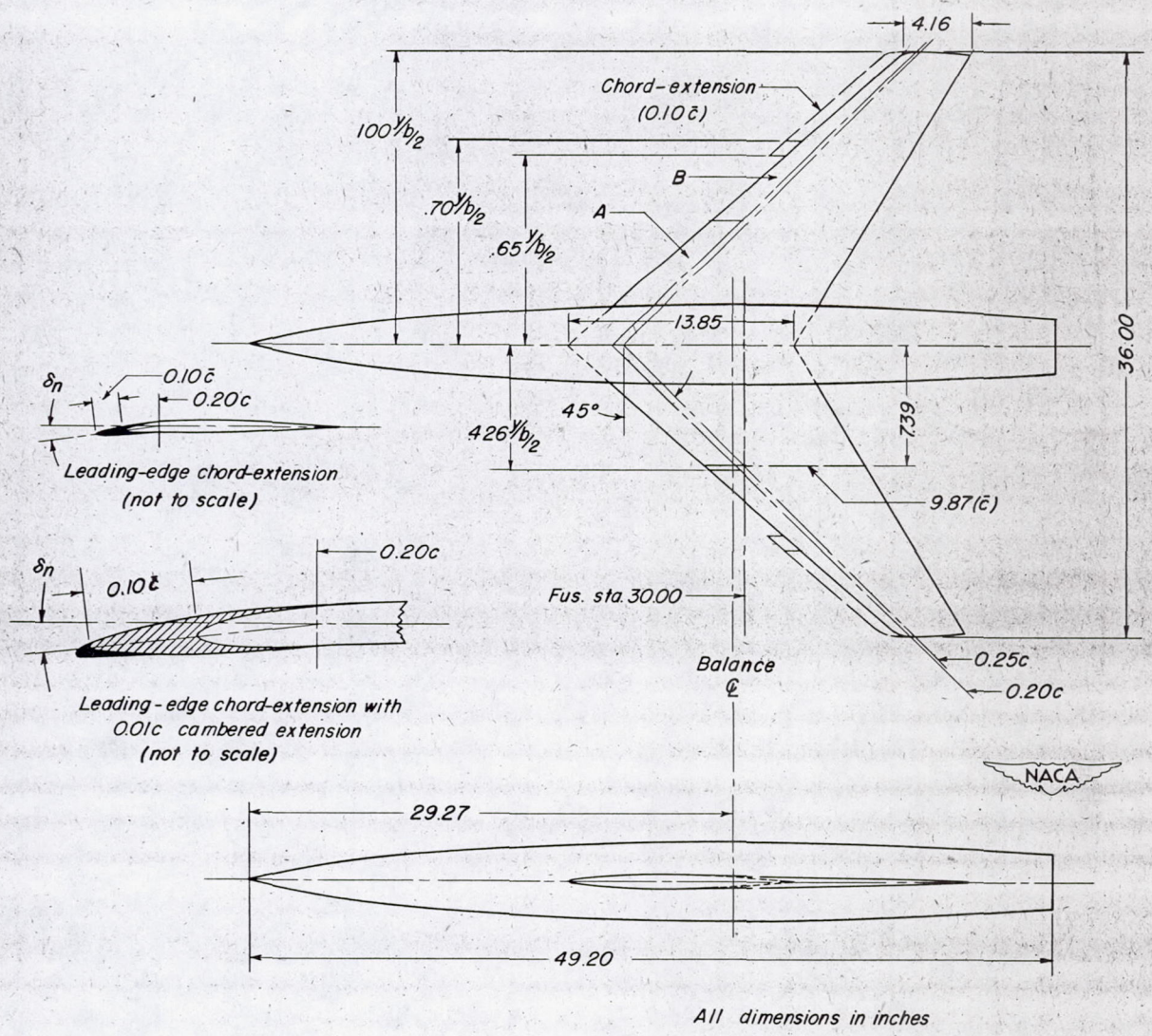

Figure 1.- Test model showing details of leading-edge flaps and chord-extensions employed.

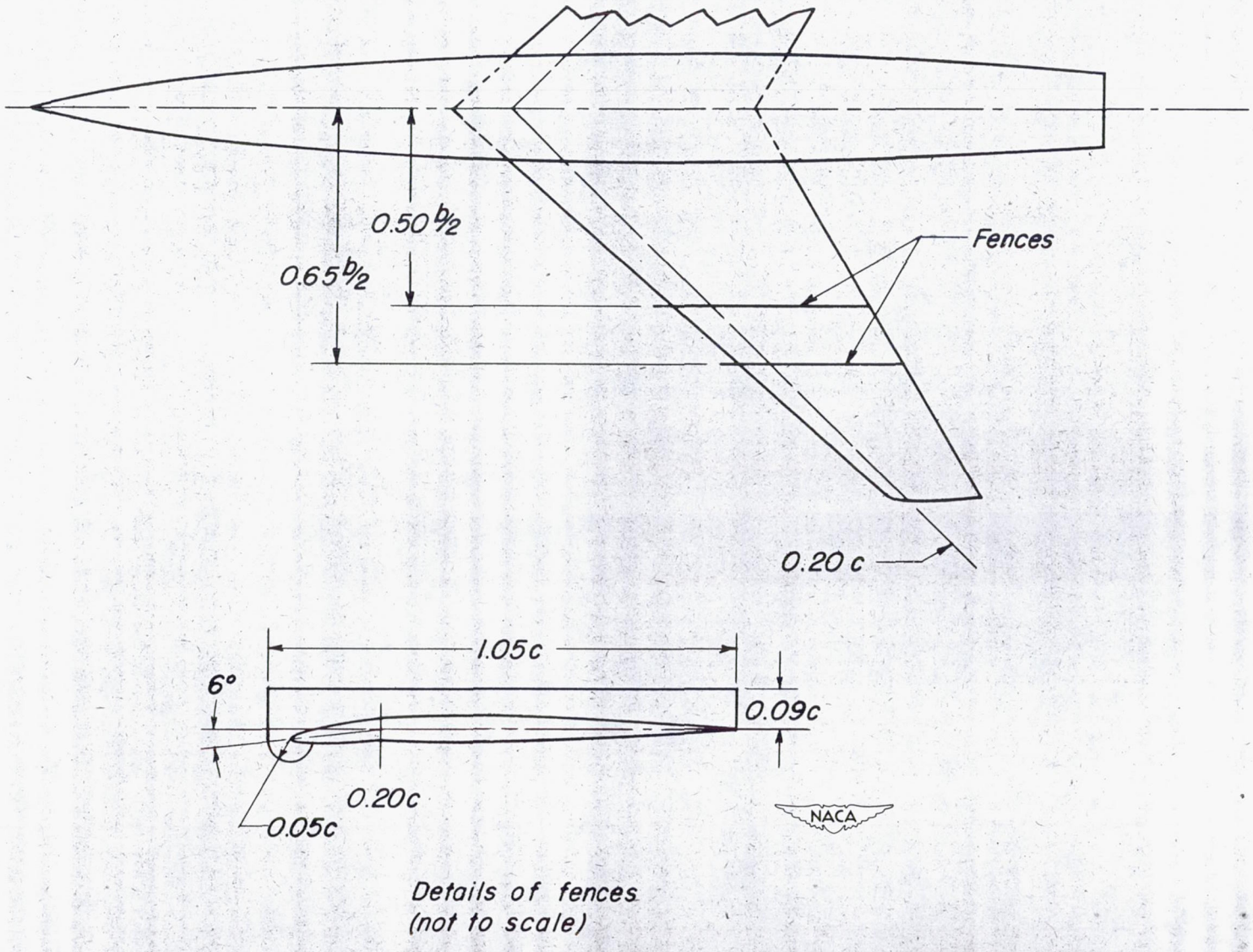

Figure 2.- Fences tested at 0.65b/2 and 0.50b/2 with full-span flap deflection of 6°.

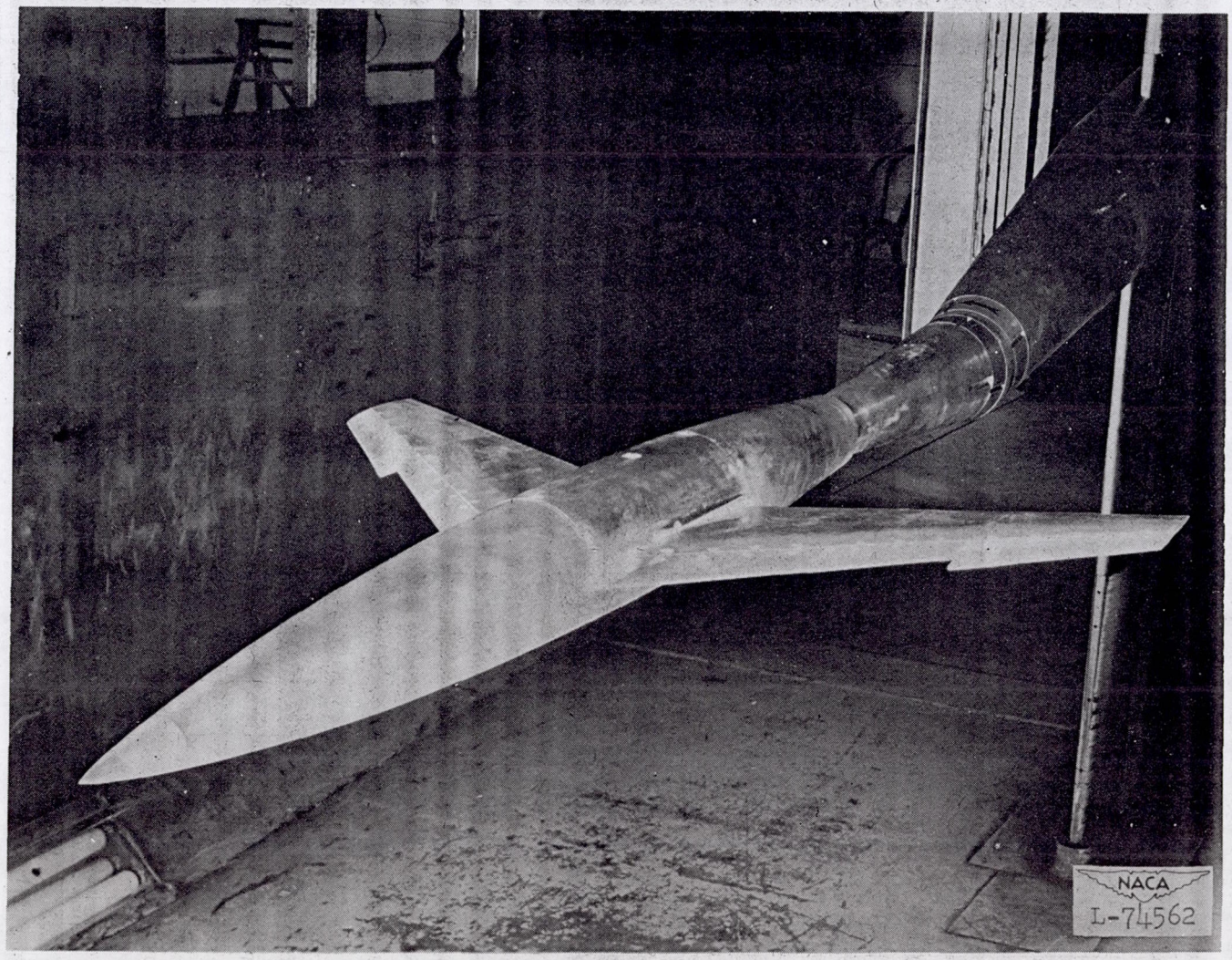

Figure 3.- View of model mounted in Langley high-speed 7- by 10-foot tunnel showing 6° full-span flap deflection with chord-extension from 0.65b/2 to tip.

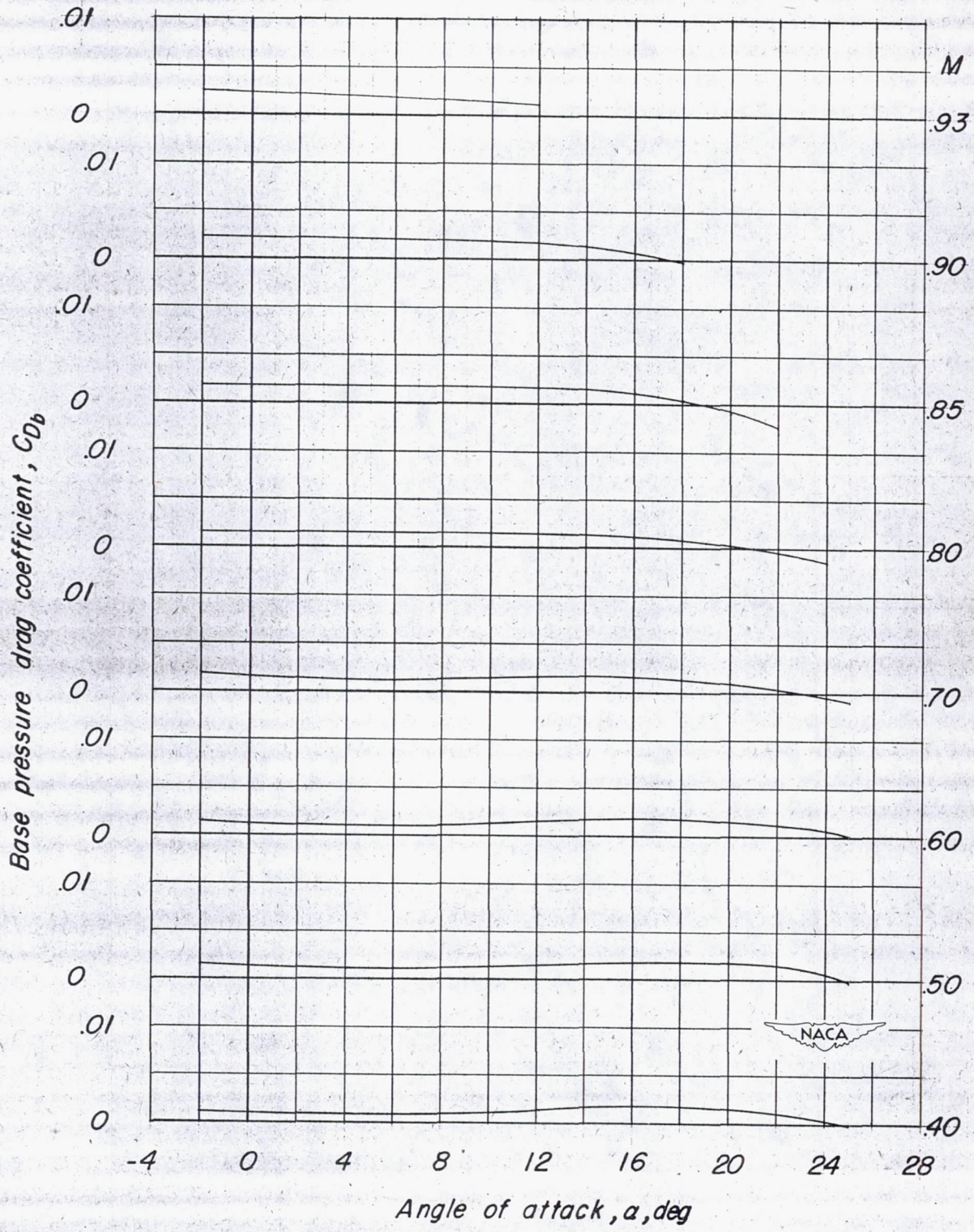

Figure 4.- Variation of base pressure drag coefficient with angle of attack and test Mach number.

CONFIDENTIAL

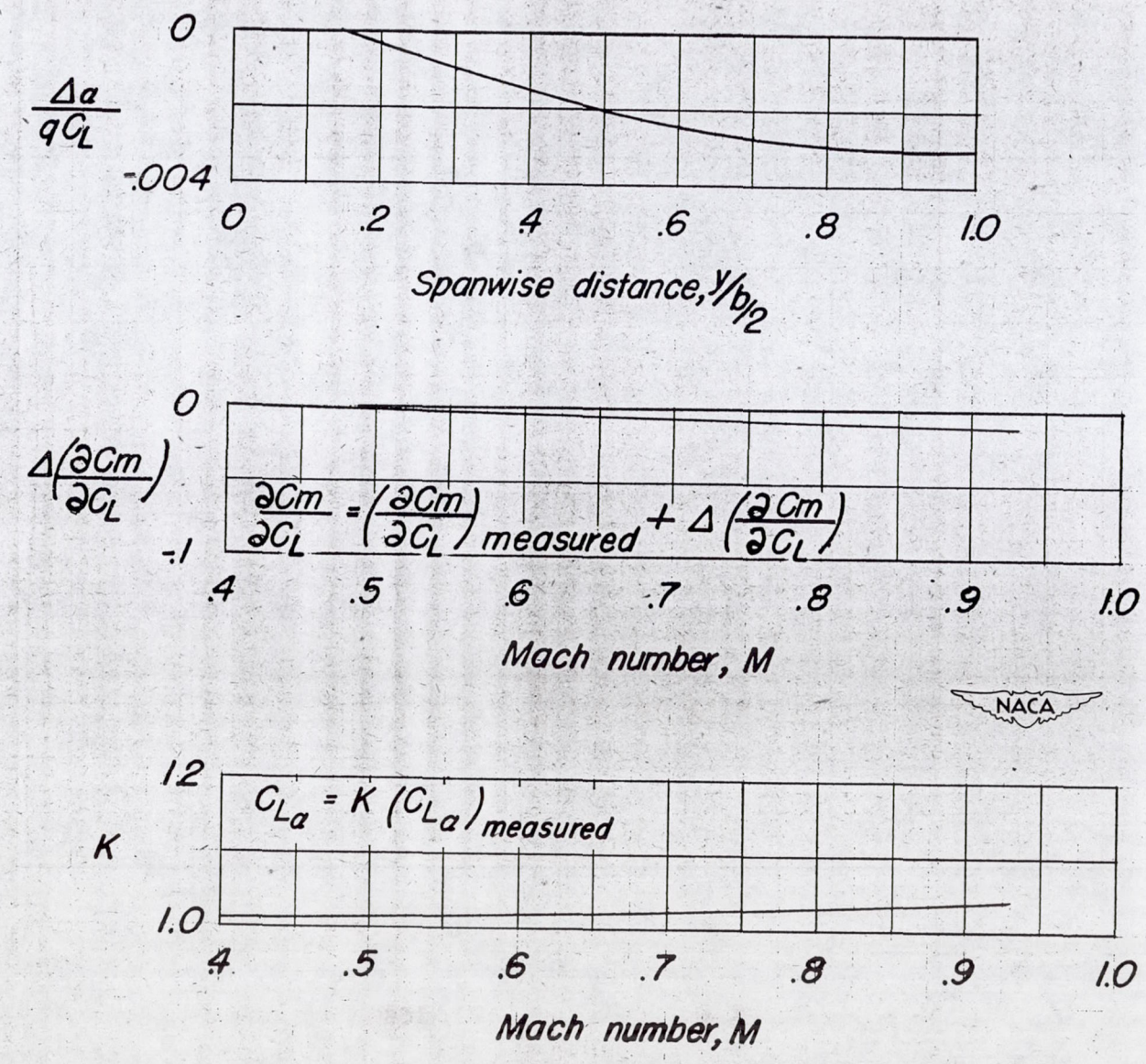

Figure 5.- Correction factors for the effects of aeroelastic distortion.

CONFIDENTIAL

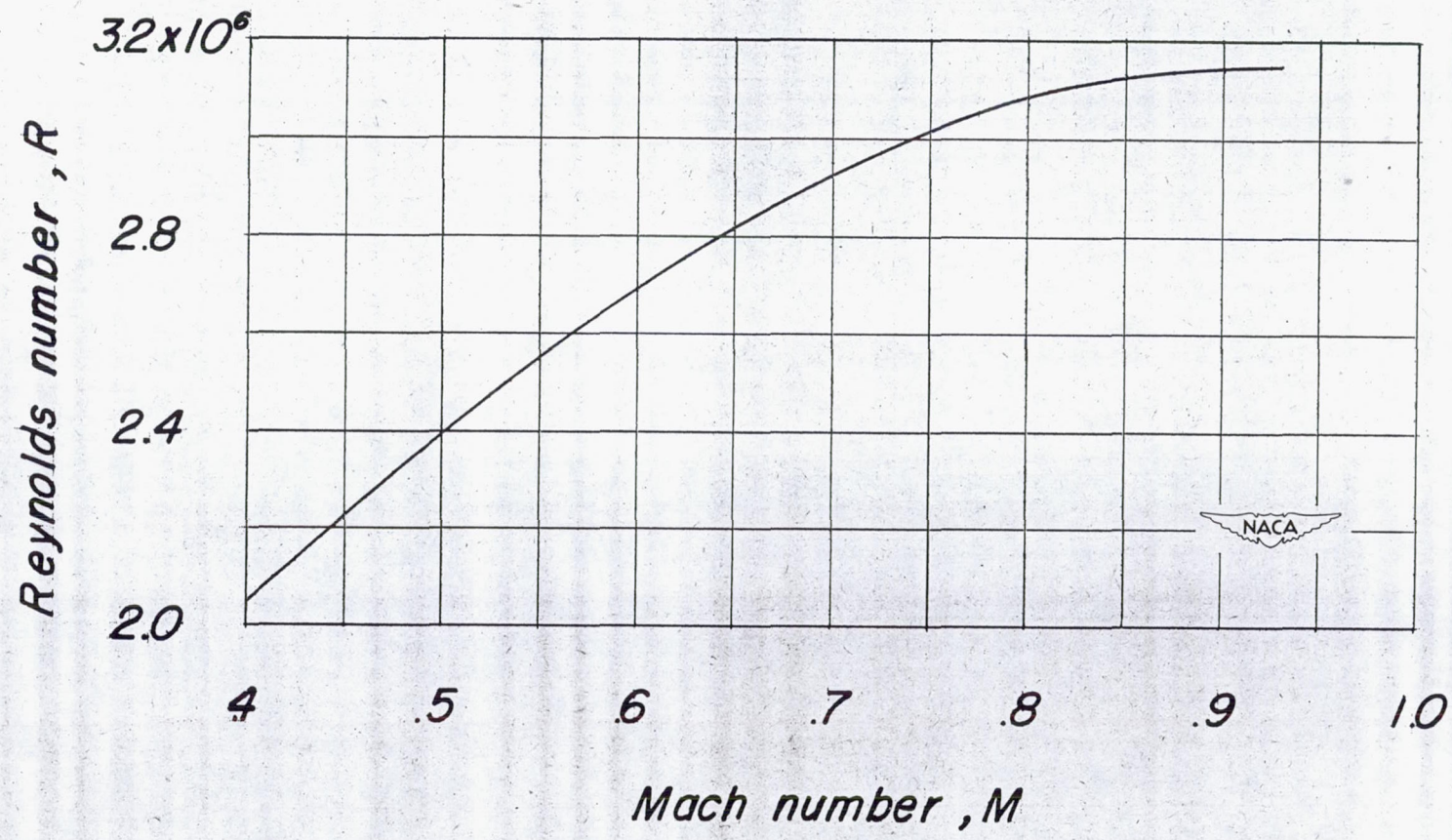

Figure 6.- Variation of mean test Reynolds number with Mach number.

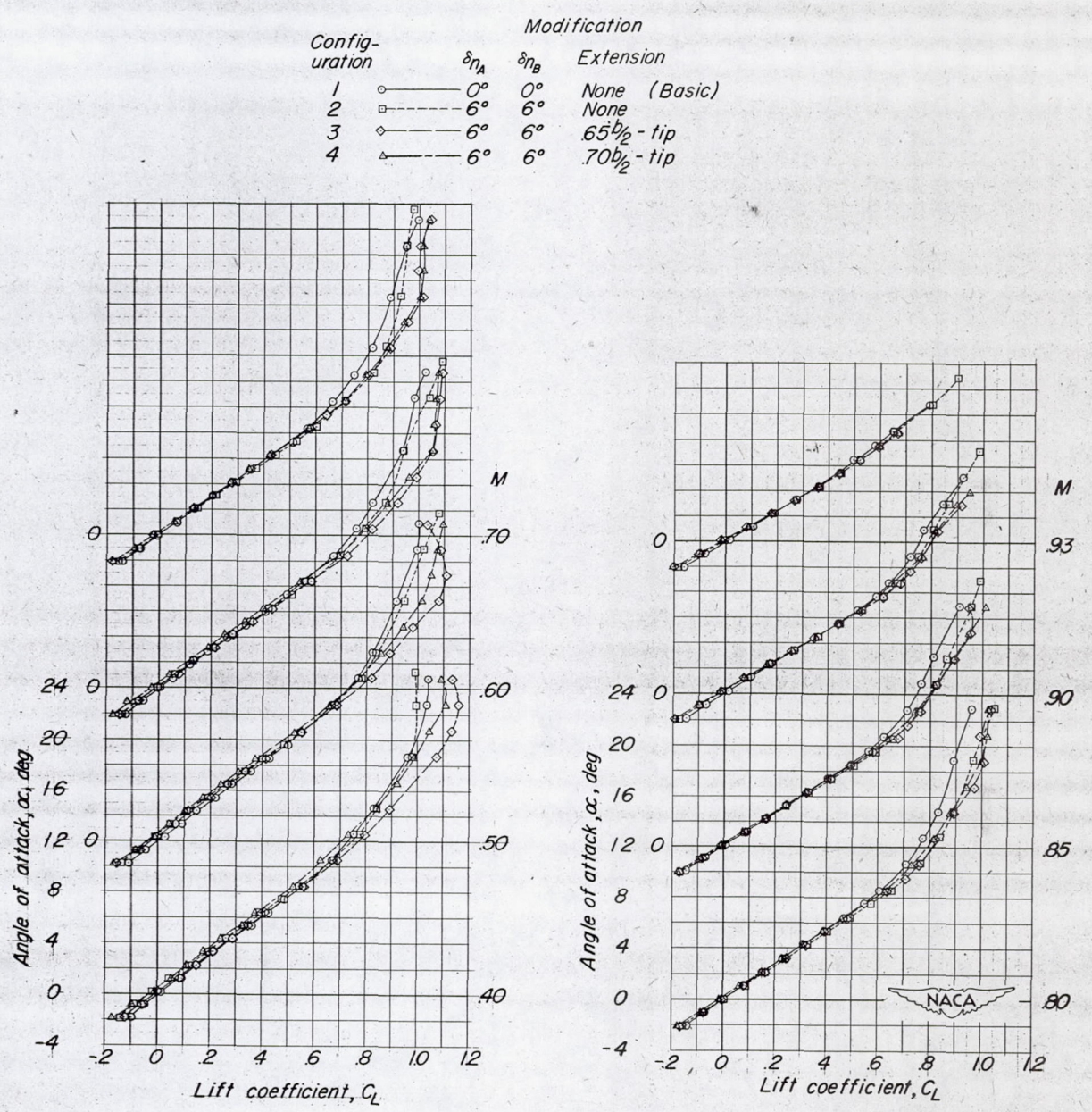

(a) α plotted against C_L.

Figure 7.- Aerodynamic characteristics of the wing-fuselage combination showing effects of leading-edge flaps and 0.10$\bar{c}$ chord-extensions.

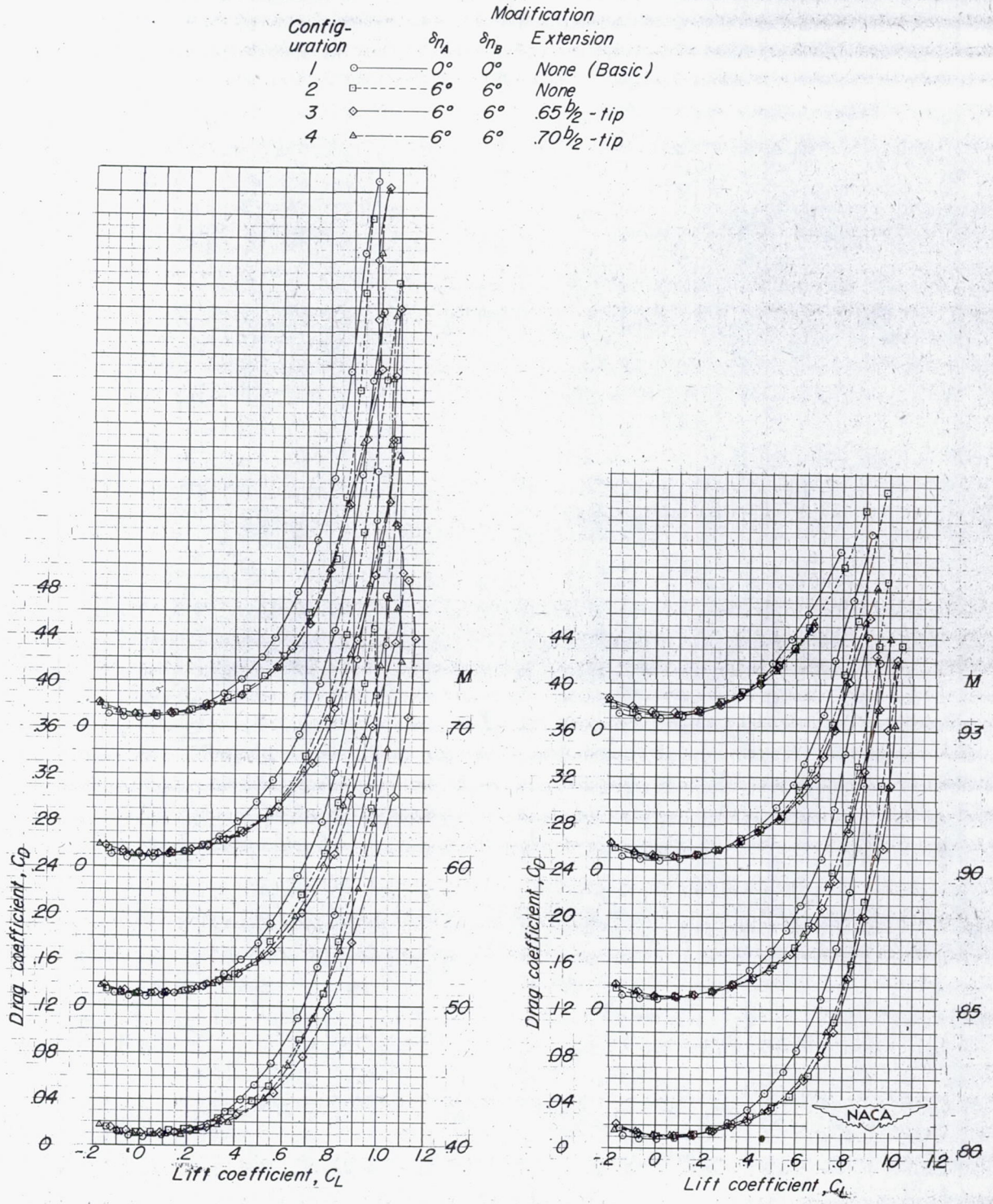

(b) C_D plotted against C_L.

Figure 7.- Continued.

CONFIDENTIAL

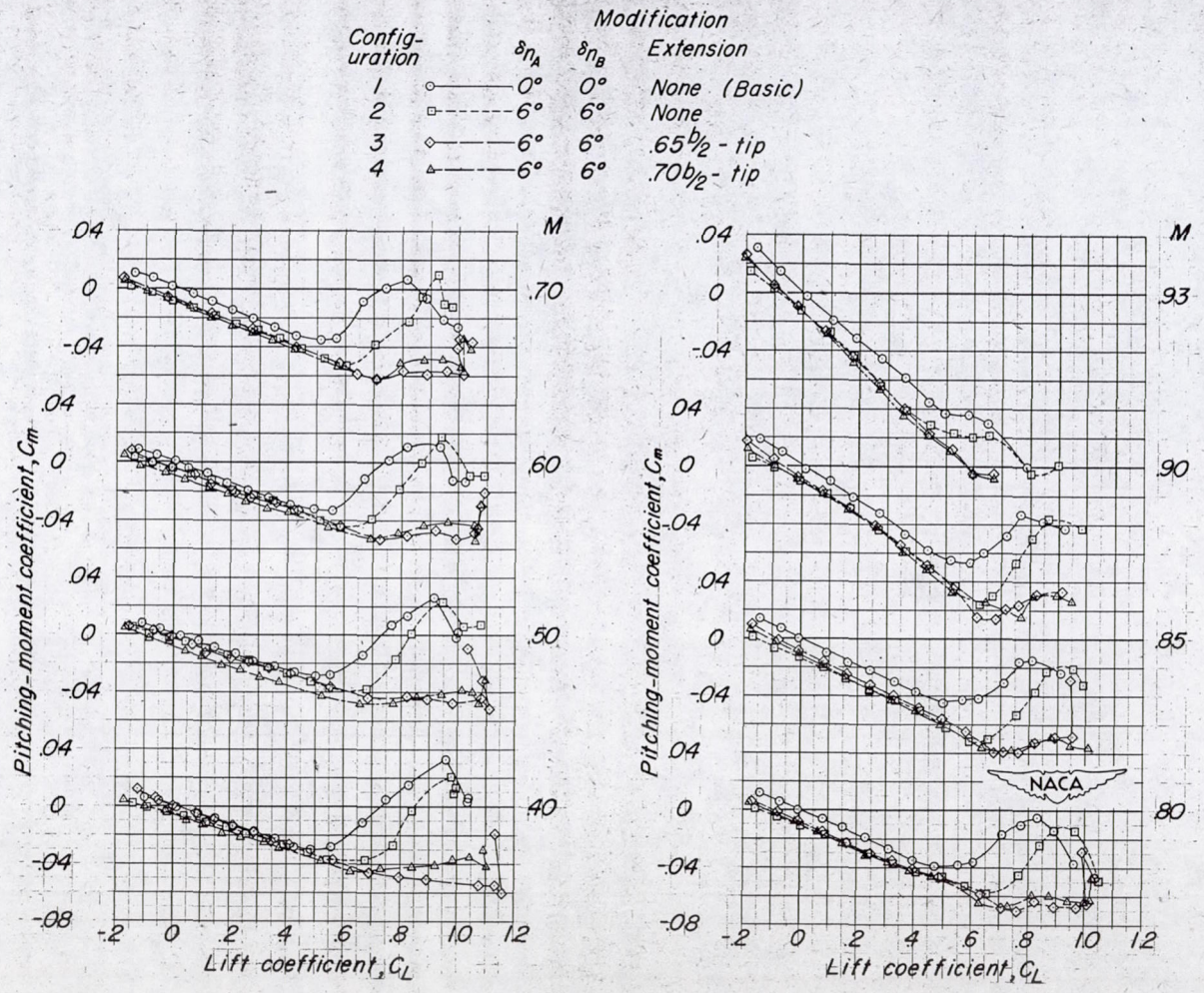

(c) C_m plotted against C_L.

Figure 7.- Continued.

CONFIDENTIAL

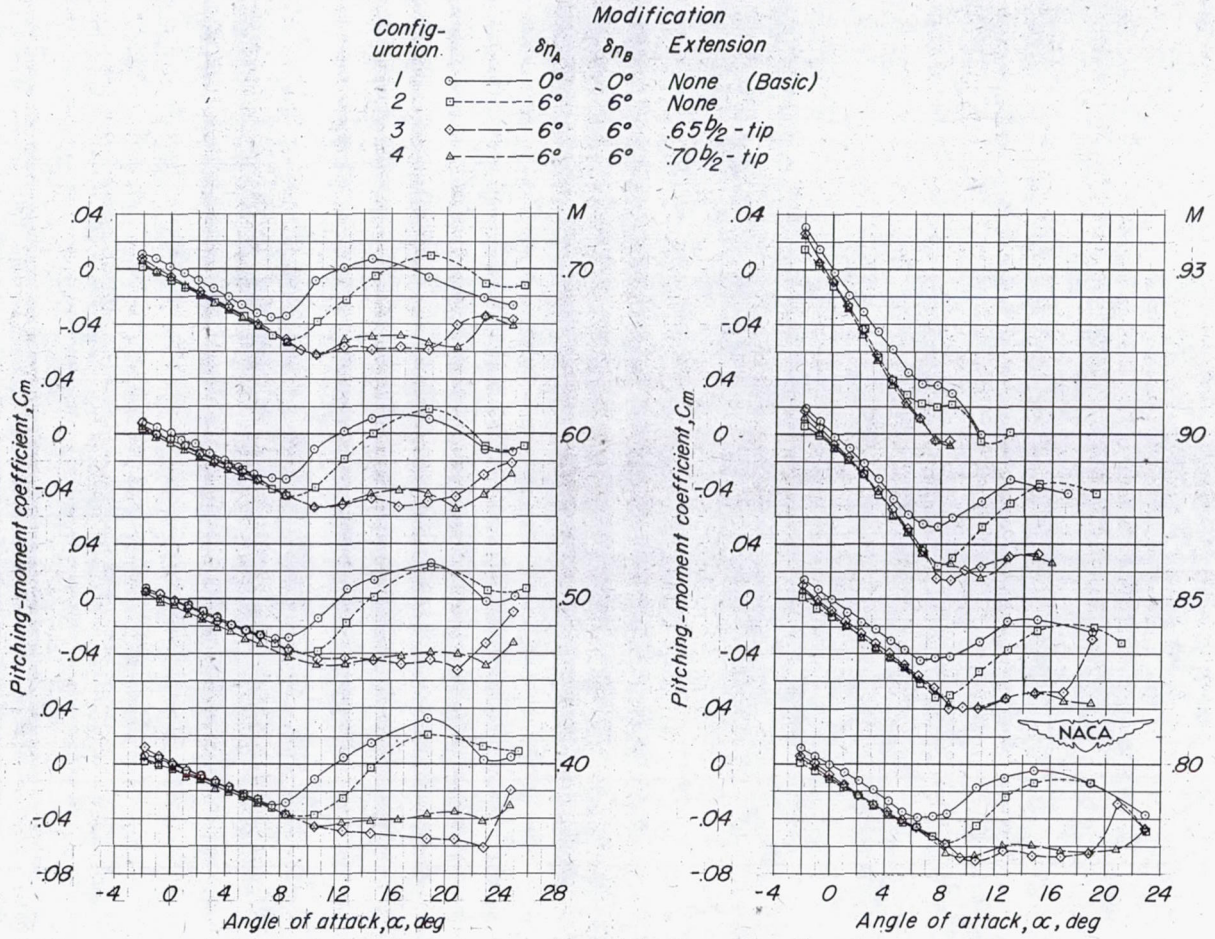

(d) C_m plotted against α.

Figure 7.- Concluded.

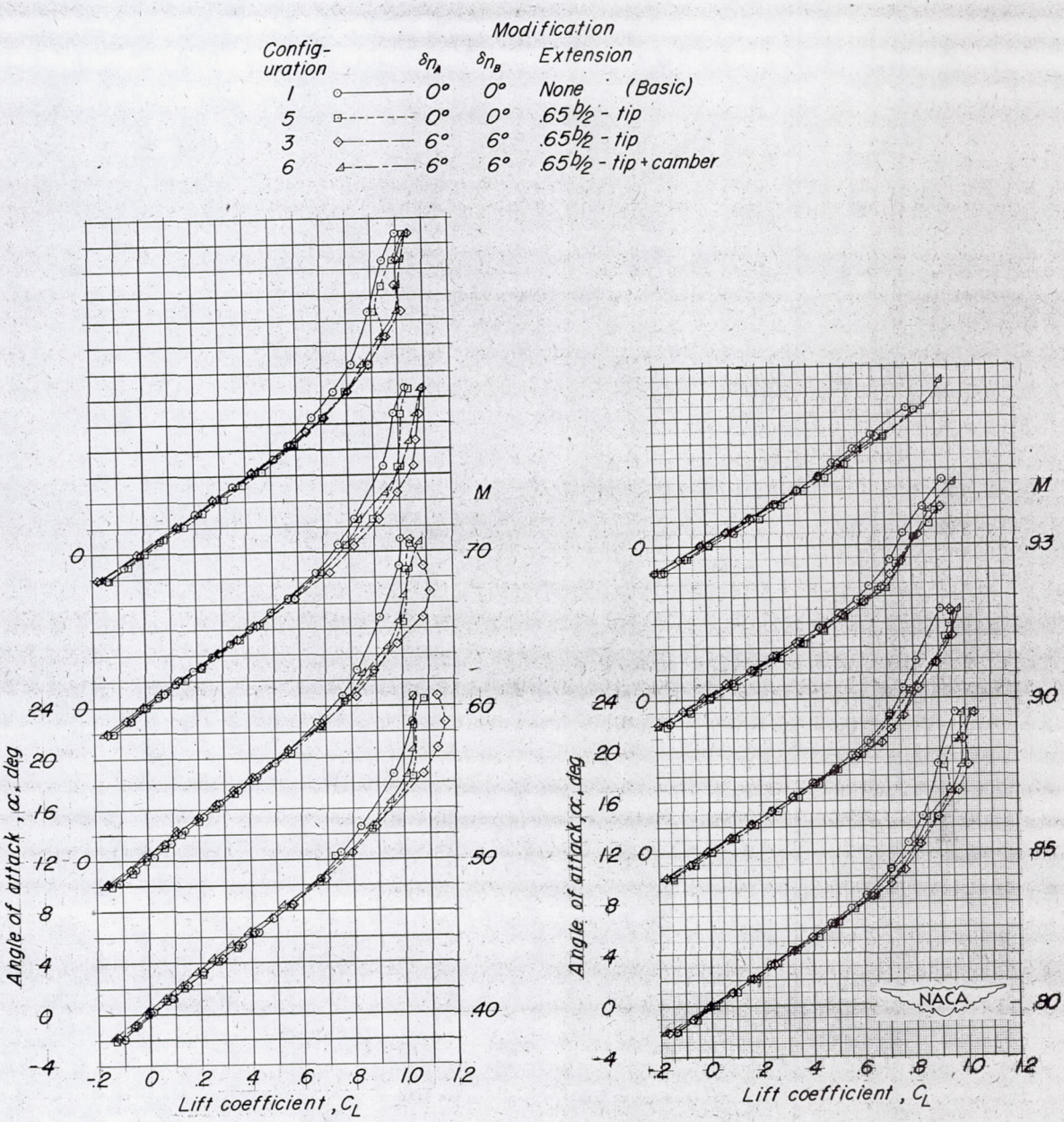

(a) α plotted against C_L.

Figure 8.- Aerodynamic characteristics of the wing-fuselage combination showing effects of 0.10$\bar{c}$ chord-extension alone and 0.10$\bar{c}$ chord-extension with camber added to leading edge.

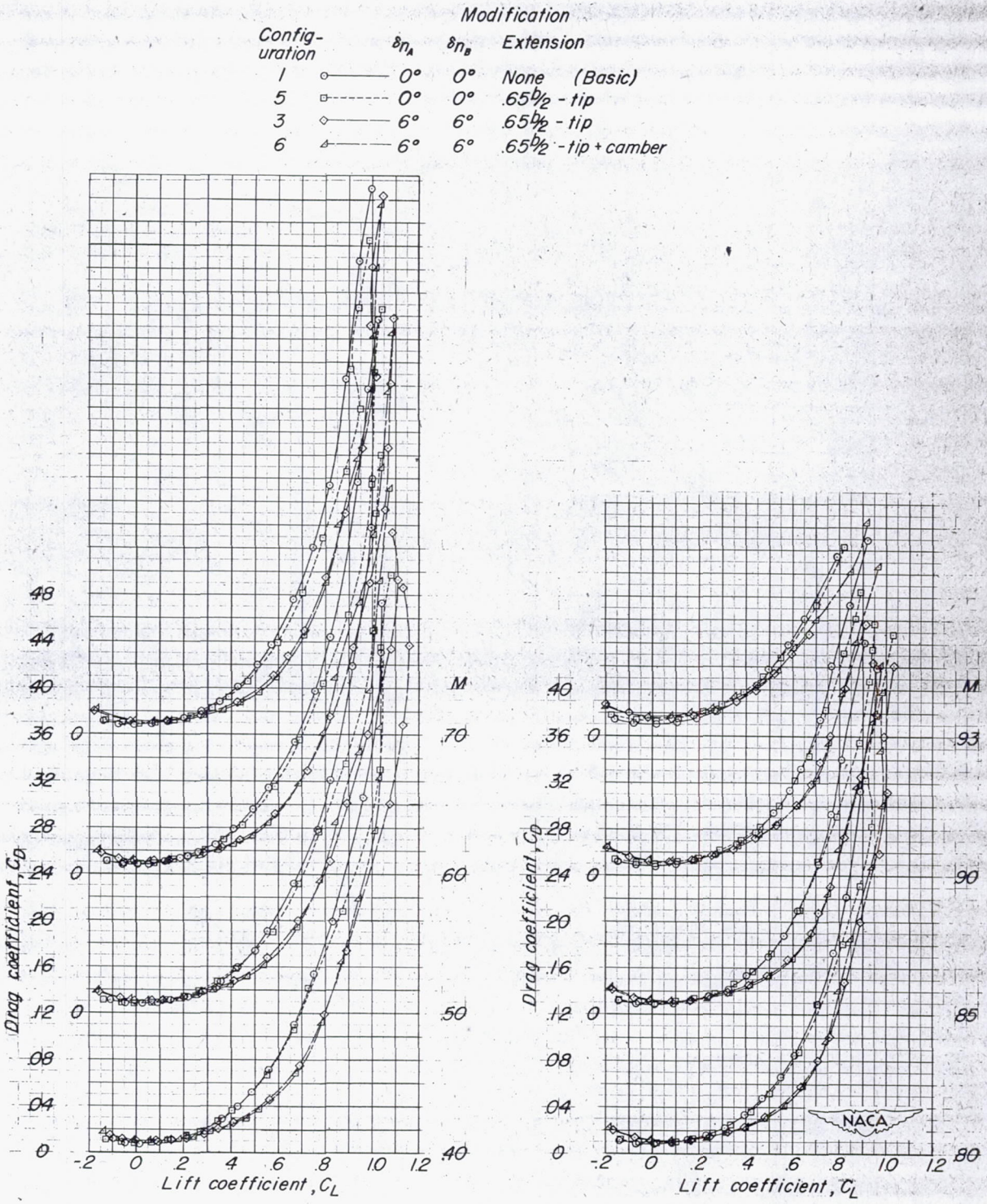

(b) C_D plotted against C_L.

Figure 8.- Continued.

CONFIDENTIAL

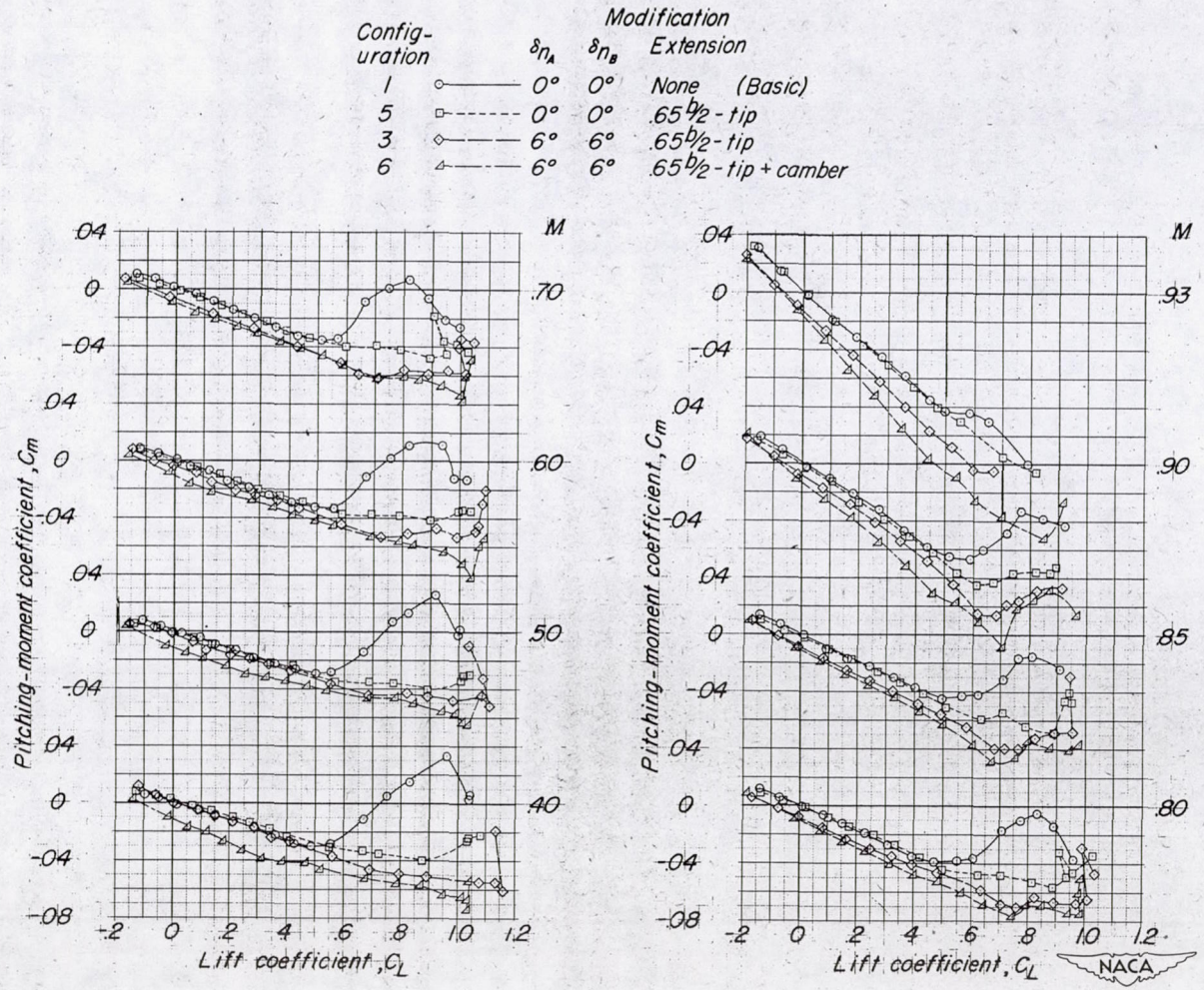

(c) C_m plotted against C_L.

Figure 8.- Continued.

CONFIDENTIAL

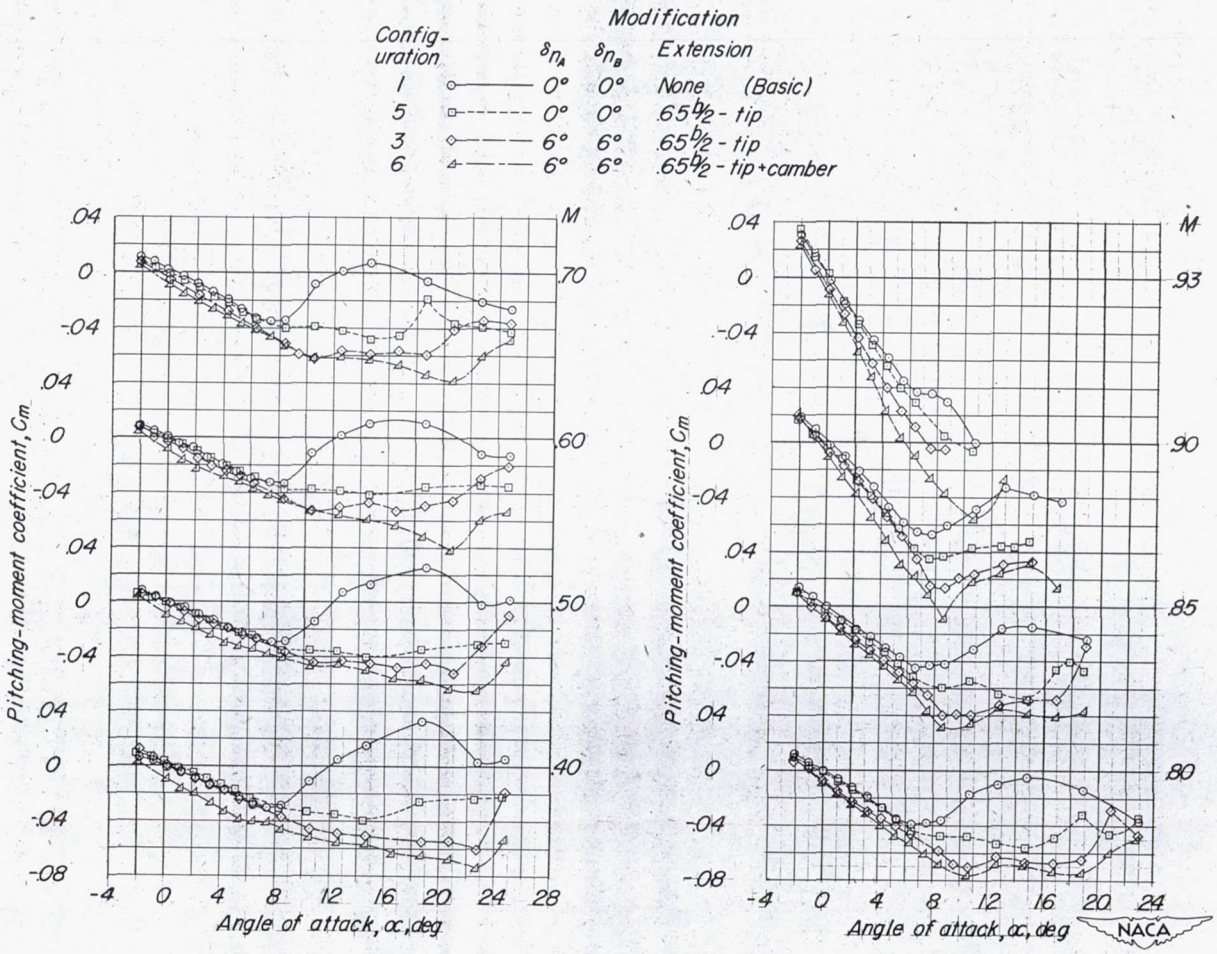

(d) C_m plotted against α.

Figure 8.- Concluded.

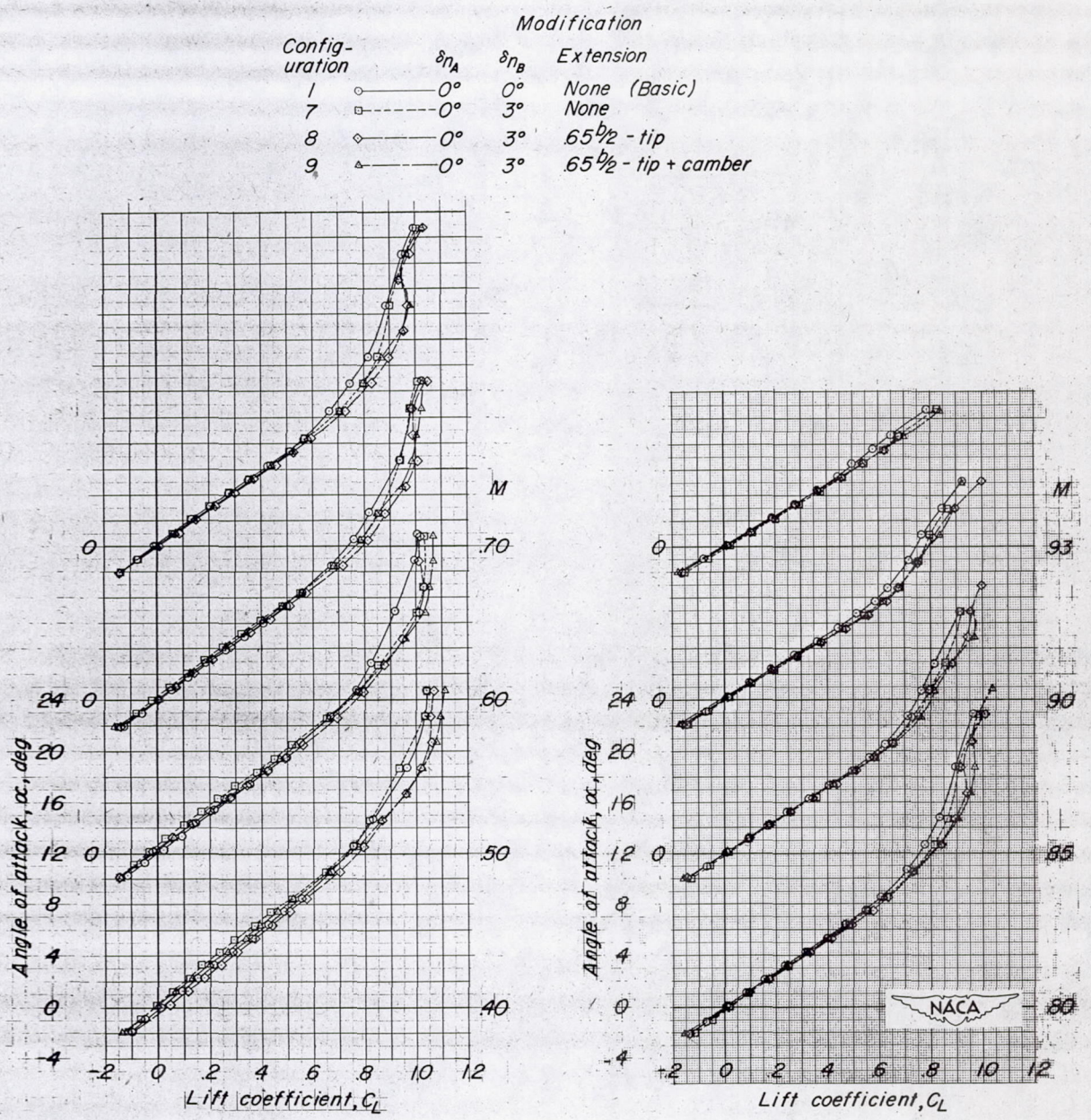

(a) α plotted against C_L.

Figure 9.- Aerodynamic characteristics of the wing-fuselage combination showing effects of partial-span leading-edge flaps, 0.10$\bar{c}$ chord-extension, and 0.10$\bar{c}$ chord-extension with camber added to leading edge.

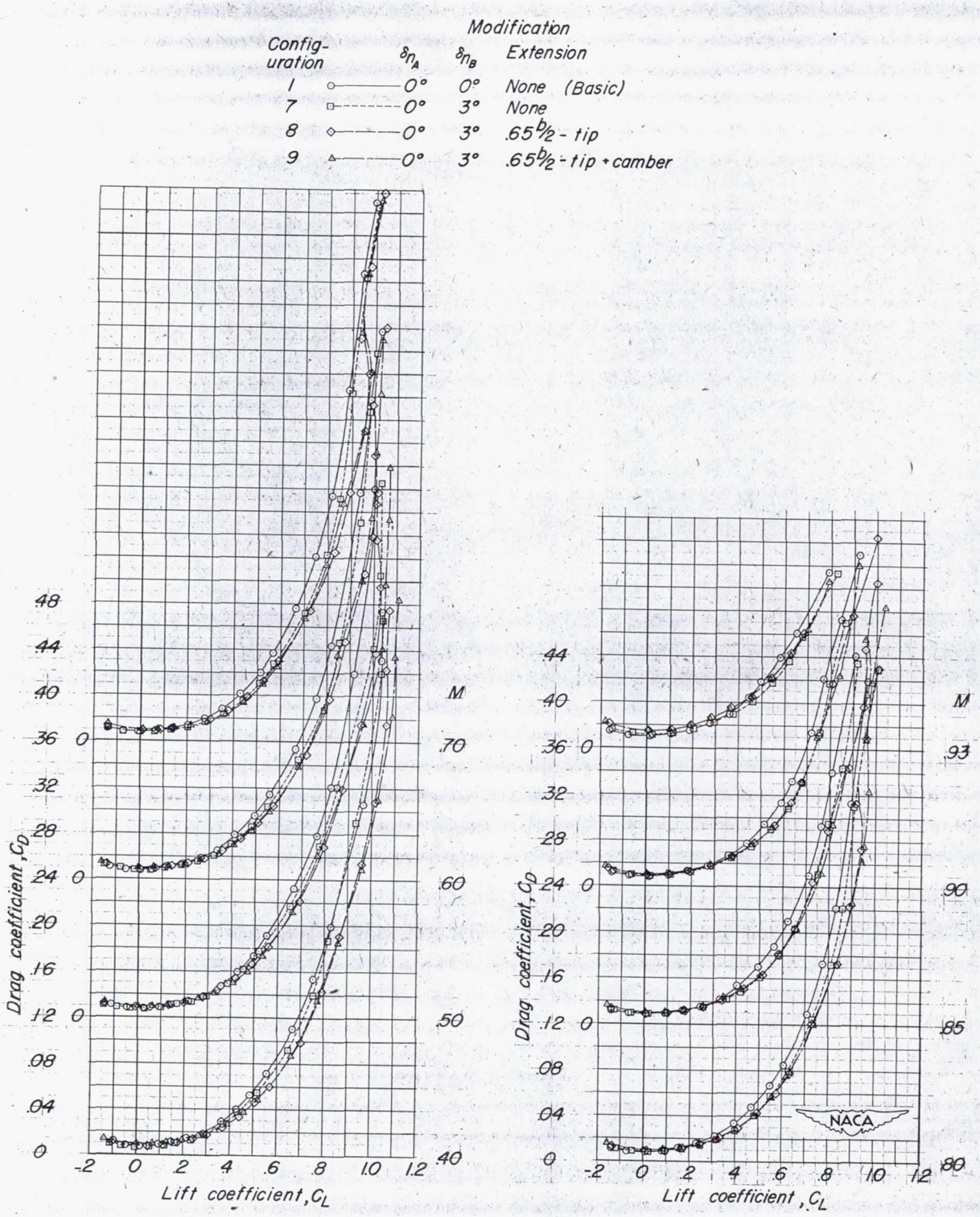

(b) C_D plotted against C_L.

Figure 9.- Continued.

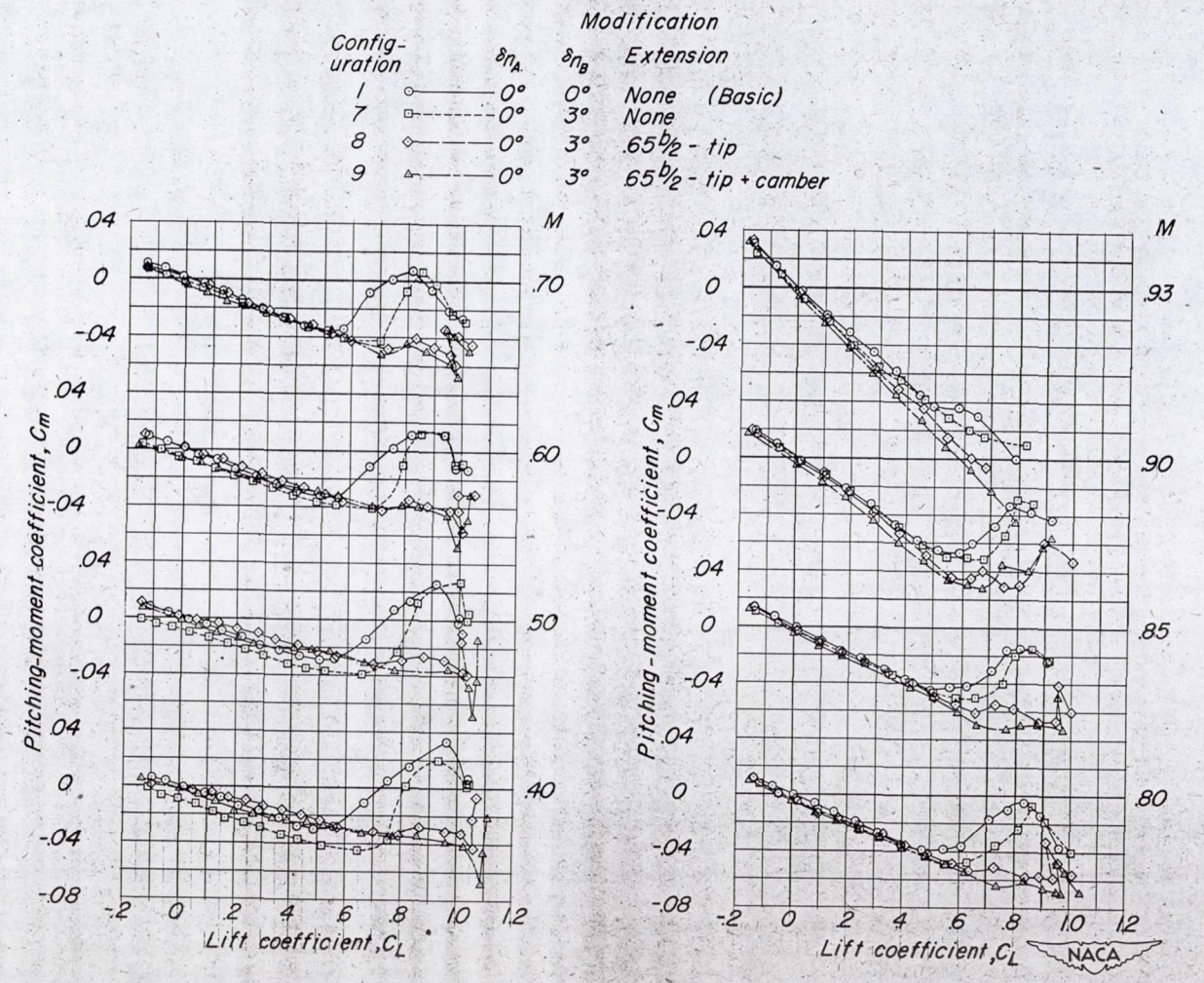

(c) C_m plotted against C_L.

Figure 9.- Continued.

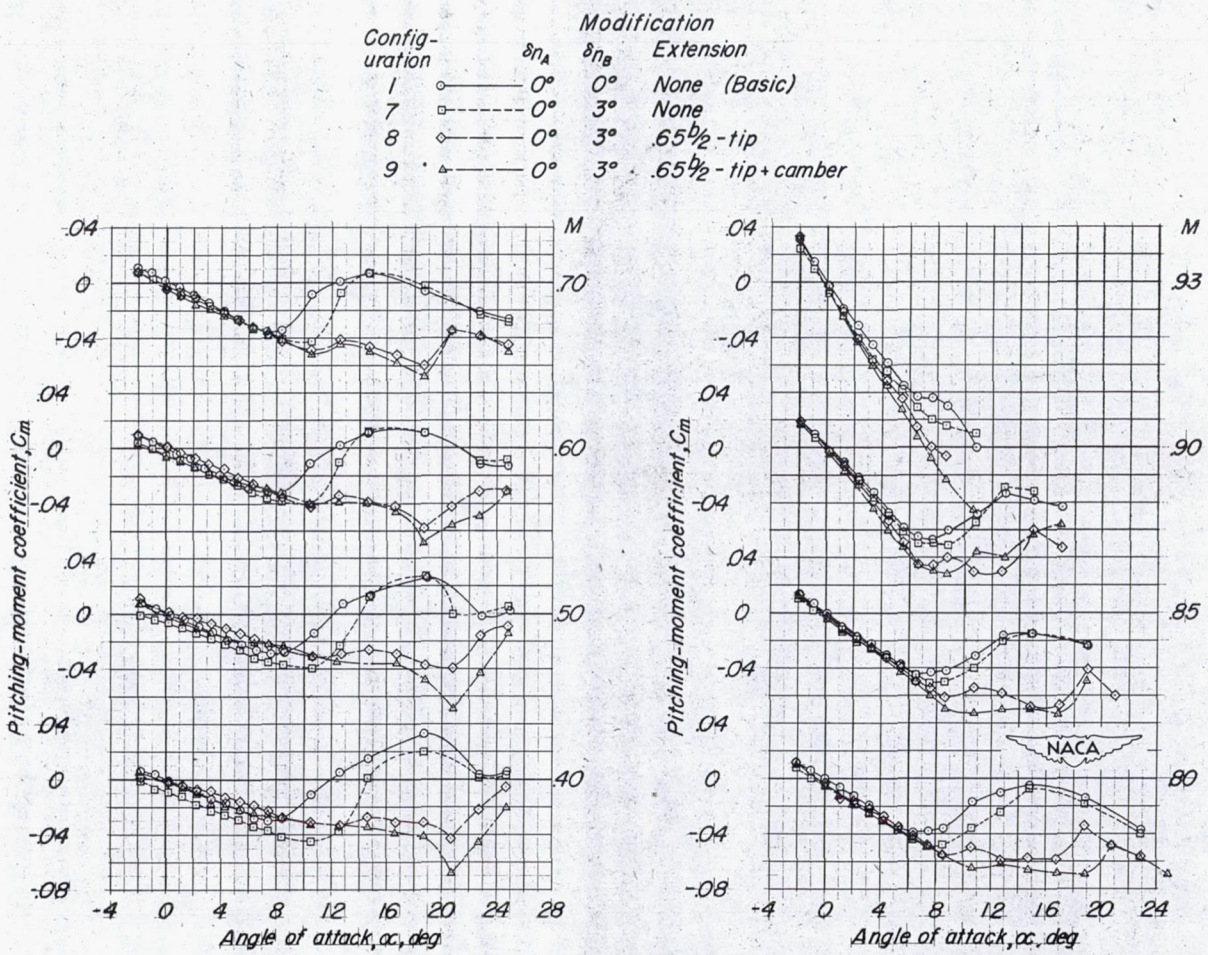

(d) C_m plotted against α.

Figure 9.- Concluded.

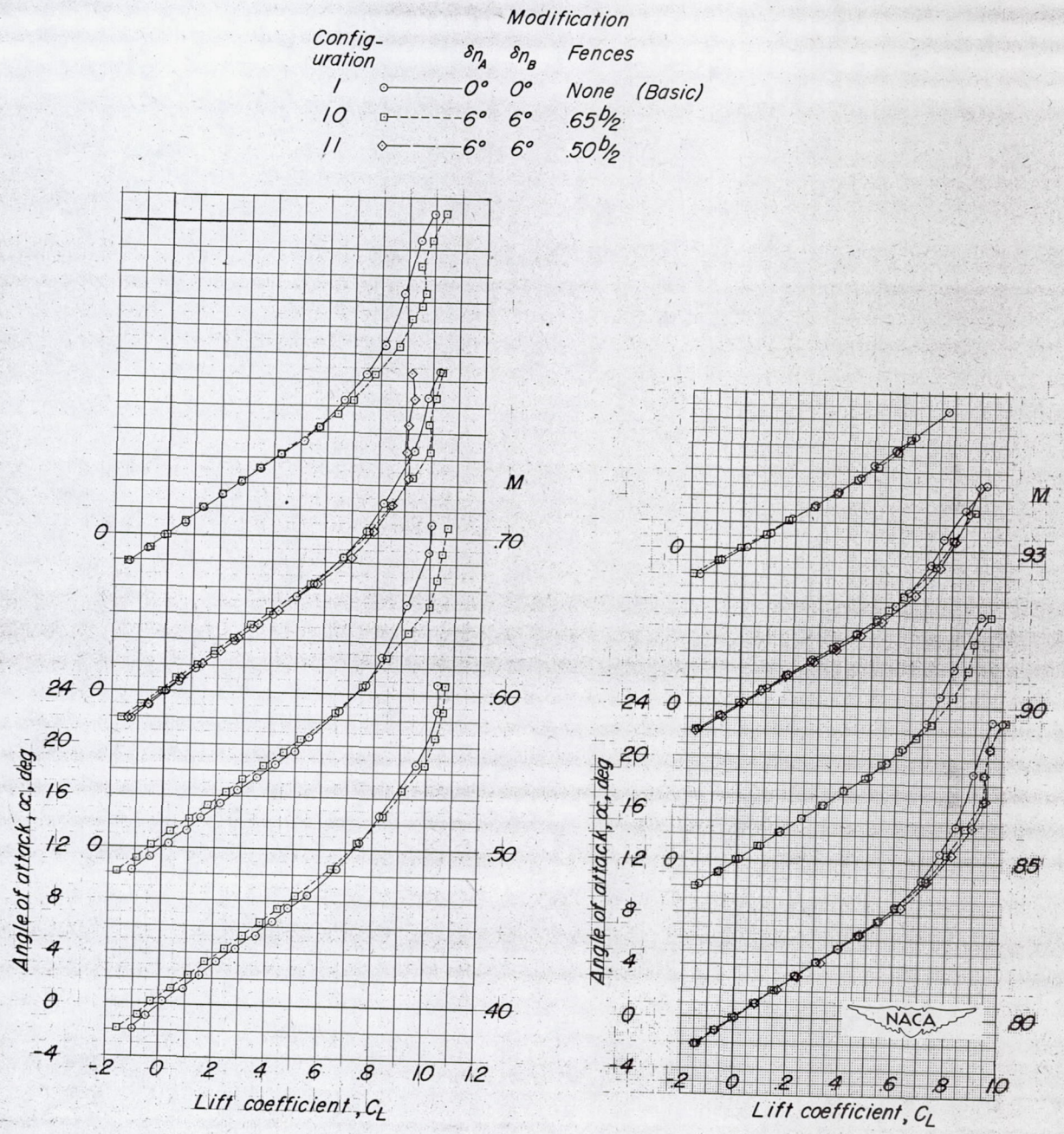

(a) α plotted against C_L.

Figure 10.- Aerodynamic characteristics of the wing-fuselage combination showing effects of fences in combination with full-span leading-edge flaps.

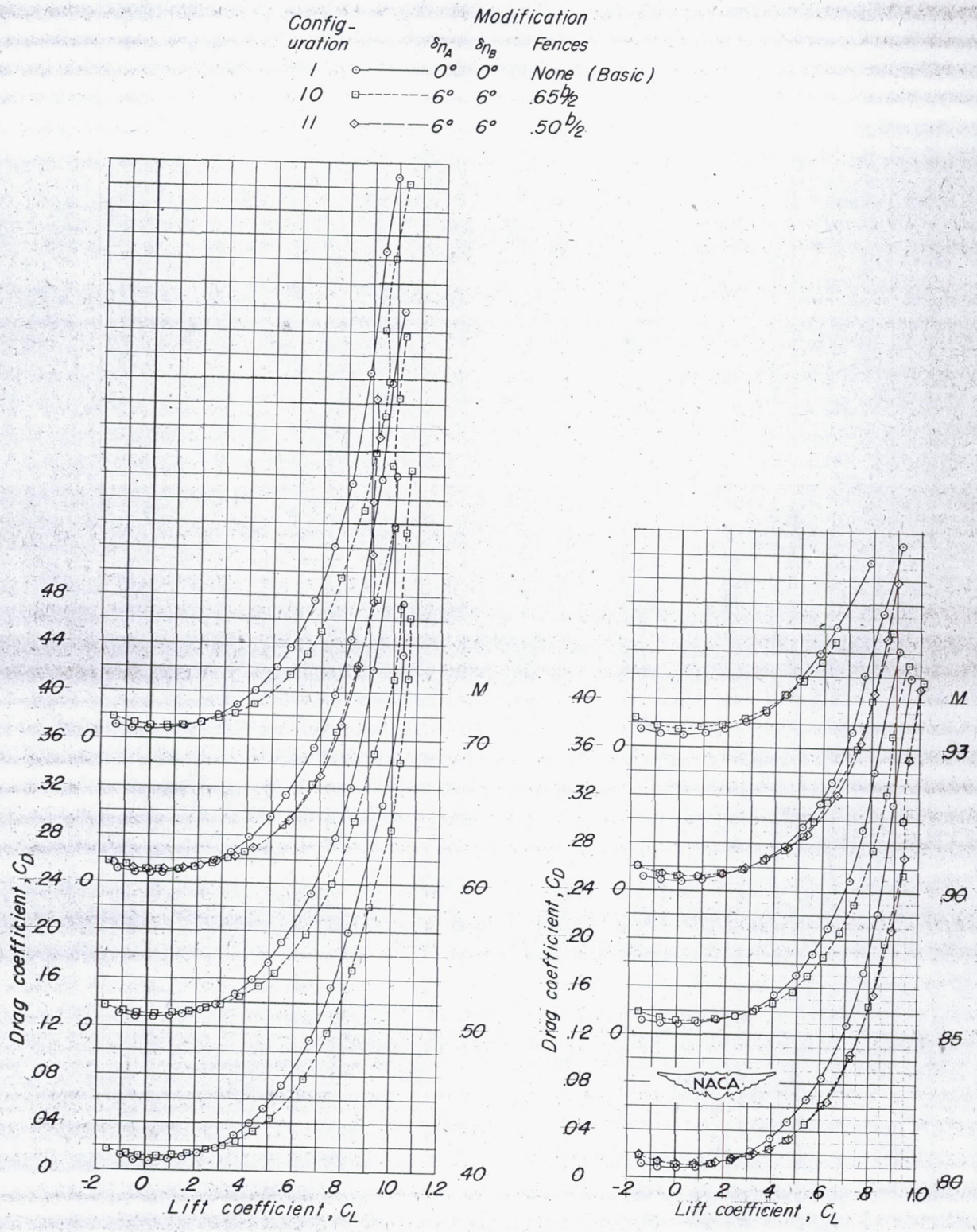

(b) C_D plotted against C_L.

Figure 10.- Continued.

CONFIDENTIAL

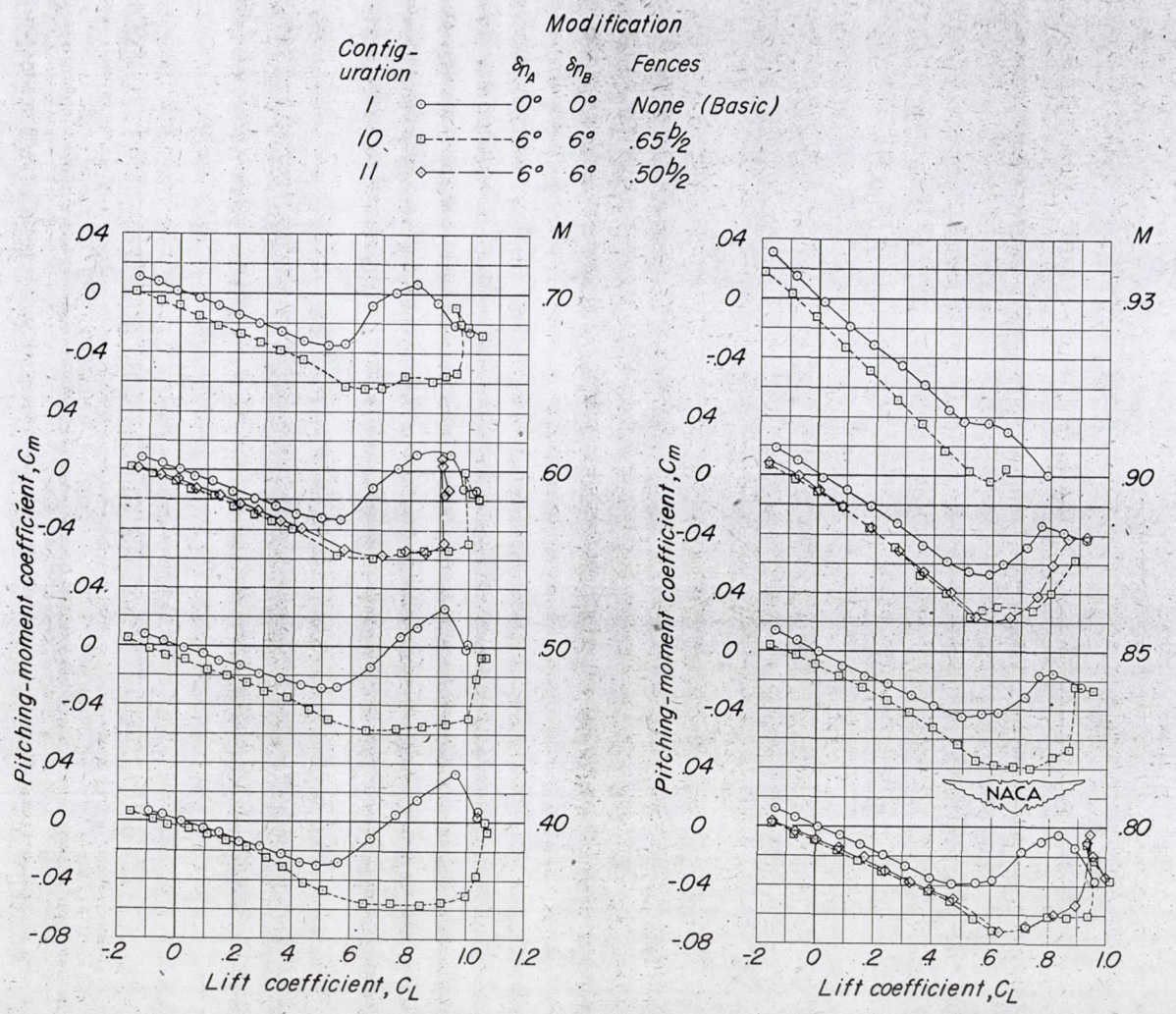

(c) C_m plotted against C_L.

Figure 10.- Continued.

CONFIDENTIAL

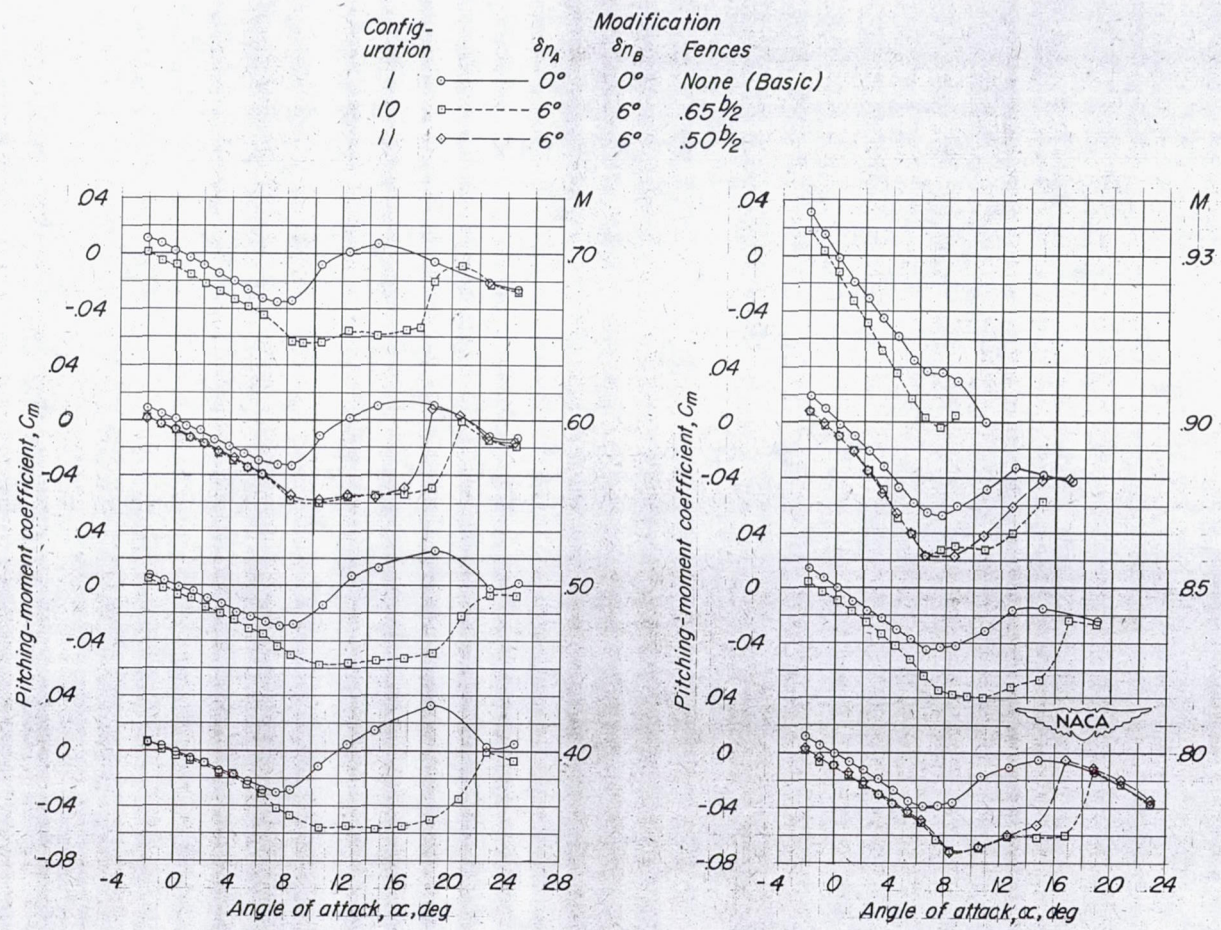

(d) C_m plotted against α.

Figure 10.- Concluded.

CONFIDENTIAL

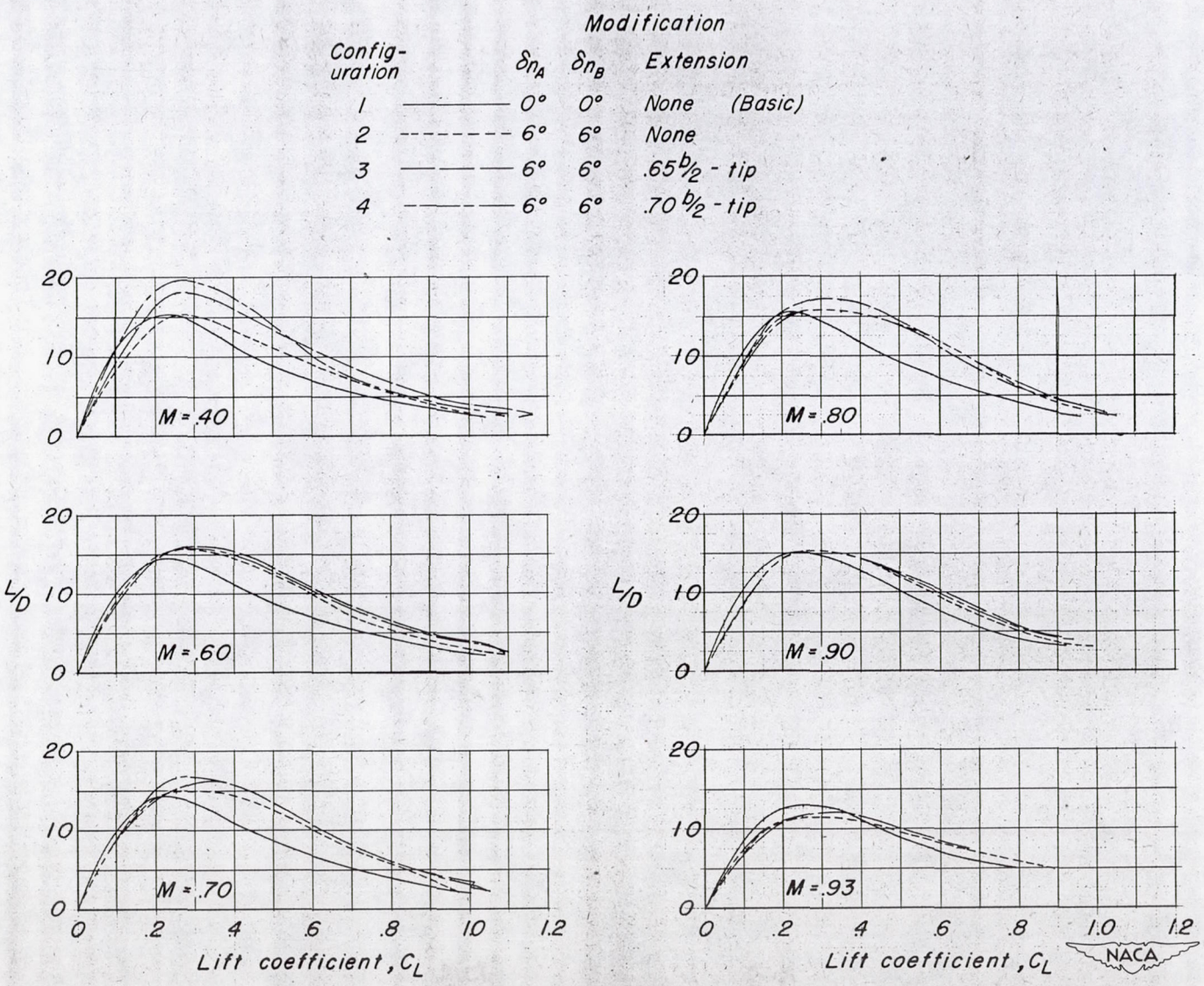

Figure 11.- Lift-drag ratios of wing-fuselage combination showing effects of leading-edge flaps and 0.10$\bar{c}$ chord-extensions.

CONFIDENTIAL

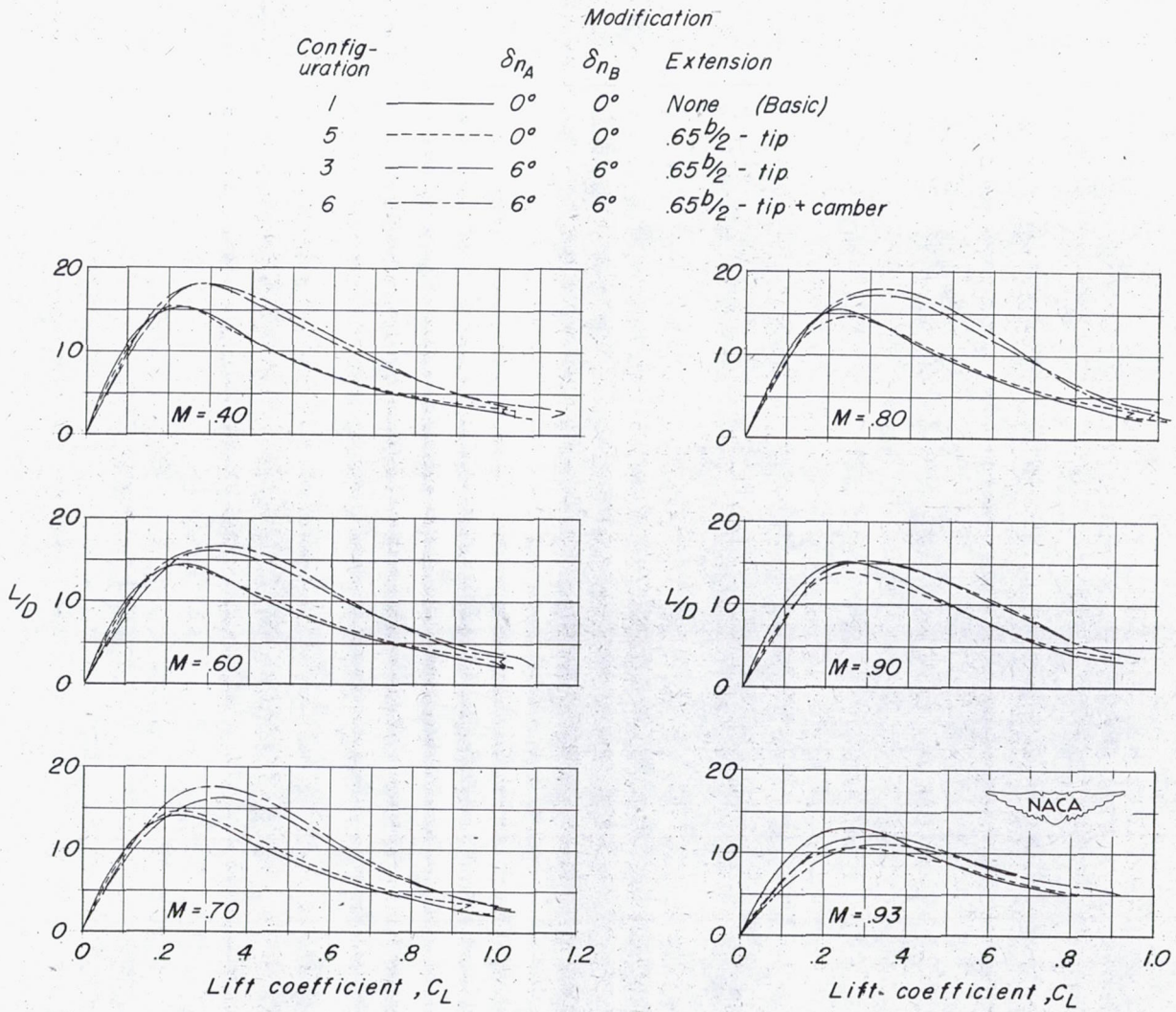

Figure 12.- Lift-drag ratios of wing-fuselage combination showing effects of 0.10$\bar{c}$ chord-extension alone and 0.10$\bar{c}$ chord-extension with camber added to leading edge.

CONFIDENTIAL

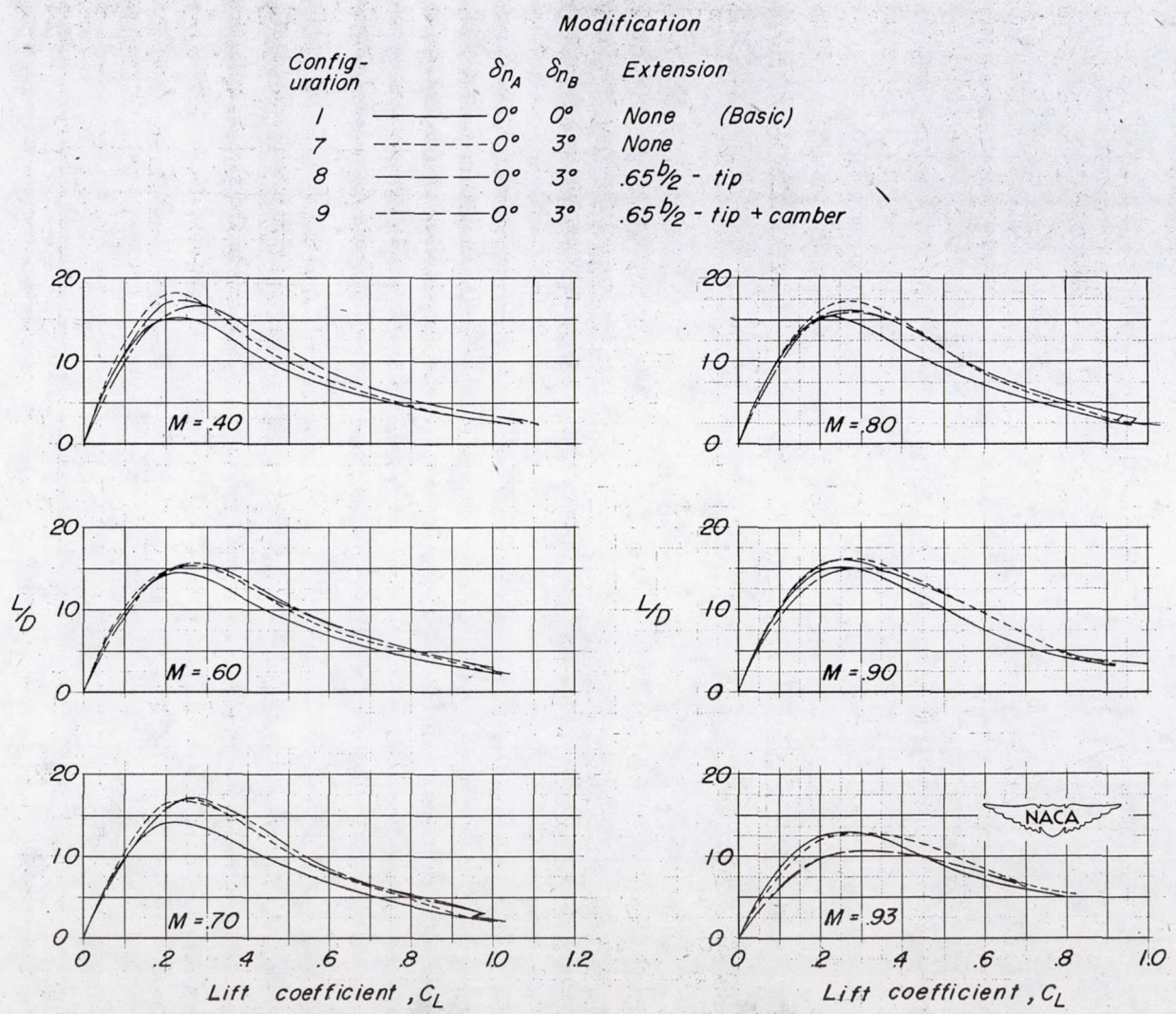

Figure 13.- Lift-drag ratios of wing-fuselage combination showing effects of partial-span leading-edge flaps, 0.10$\bar{c}$ chord-extension, and 0.10$\bar{c}$ chord-extension with camber added to leading edge.

CONFIDENTIAL

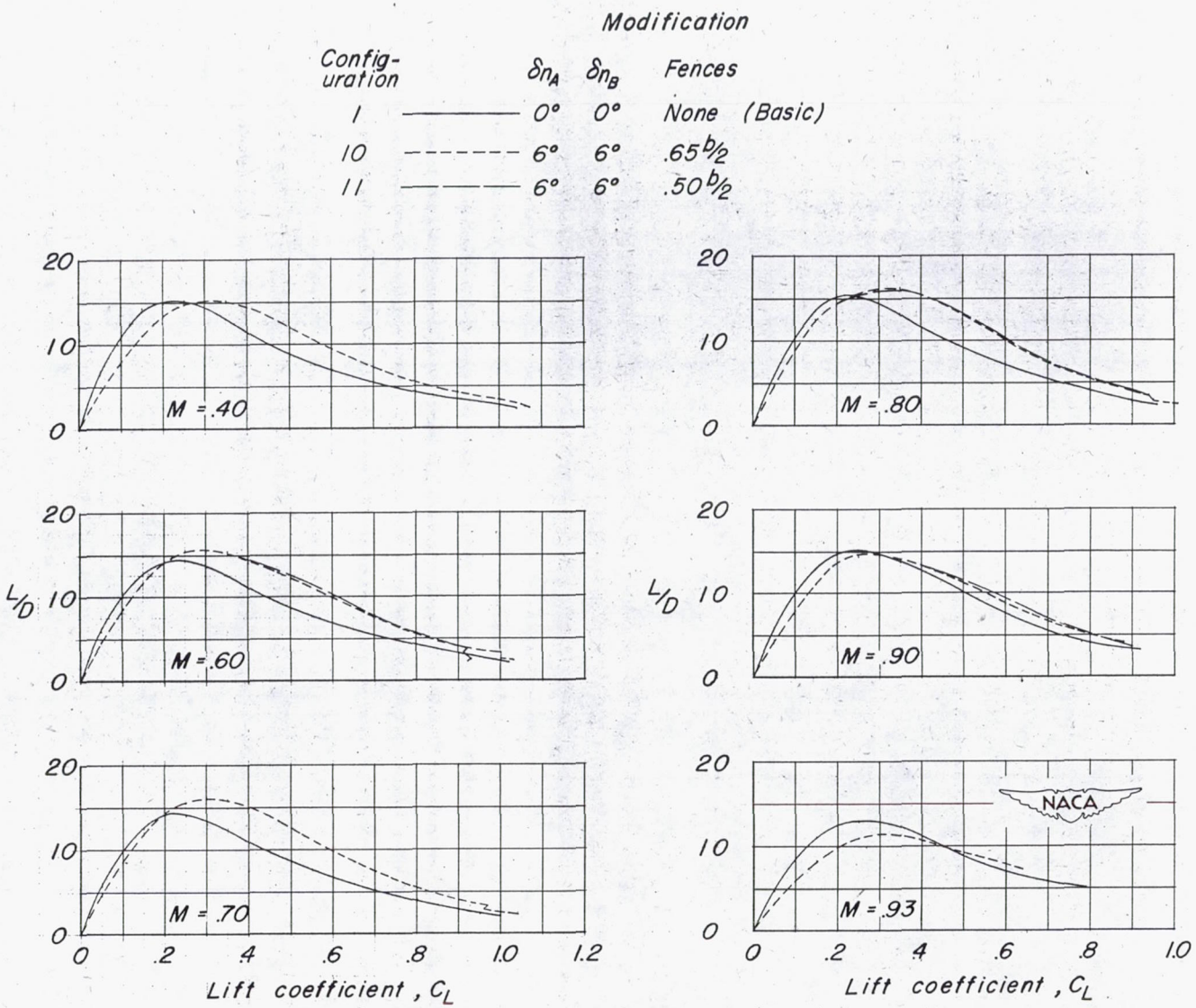

Figure 14.- Lift-drag ratios of wing-fuselage combination showing effects of fences in combination with full-span leading-edge flaps.

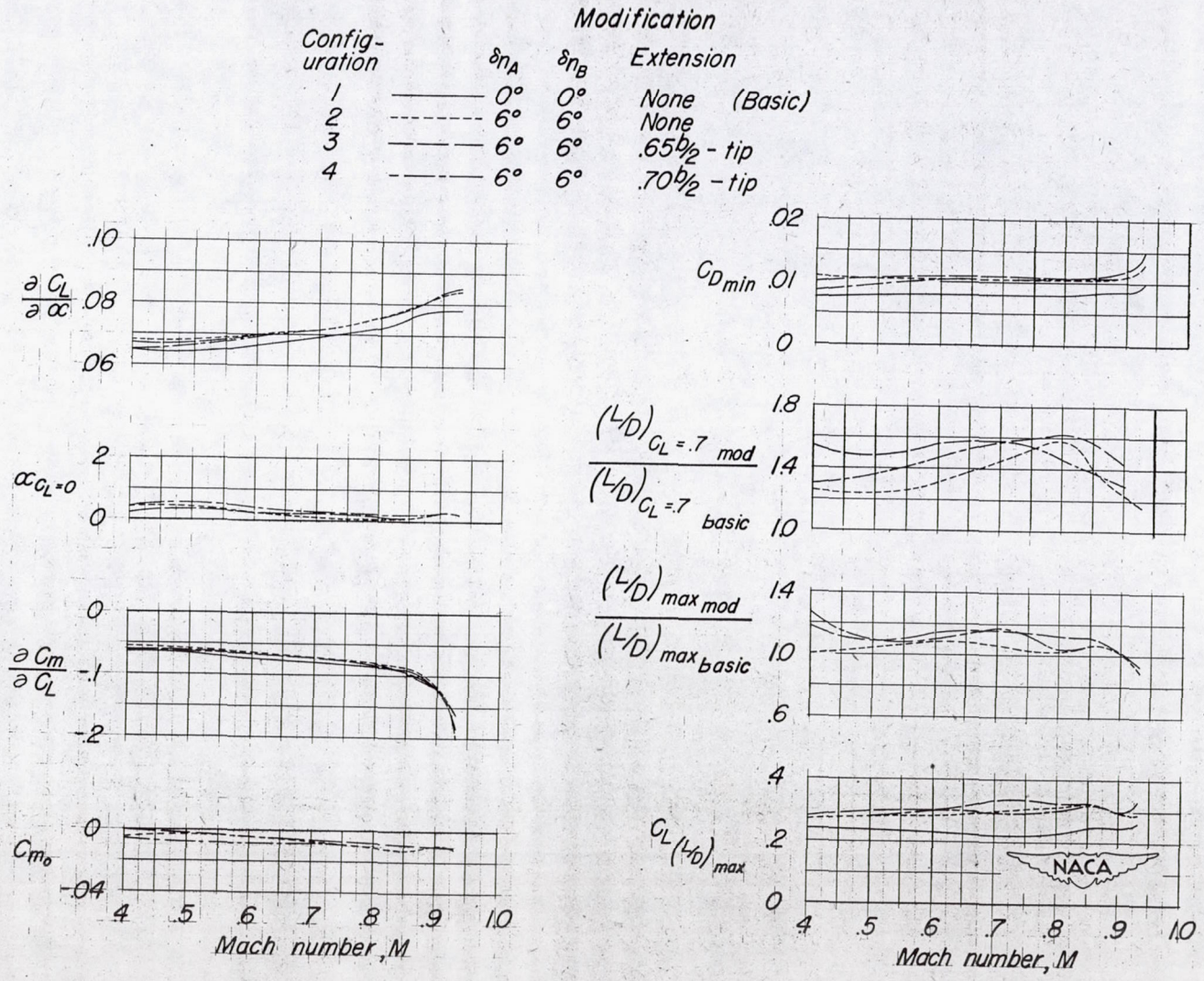

Figure 15.- Summary of aerodynamic characteristics of wing-fuselage combination showing effects of leading-edge flaps and 0.10$\bar{c}$ chord-extensions.

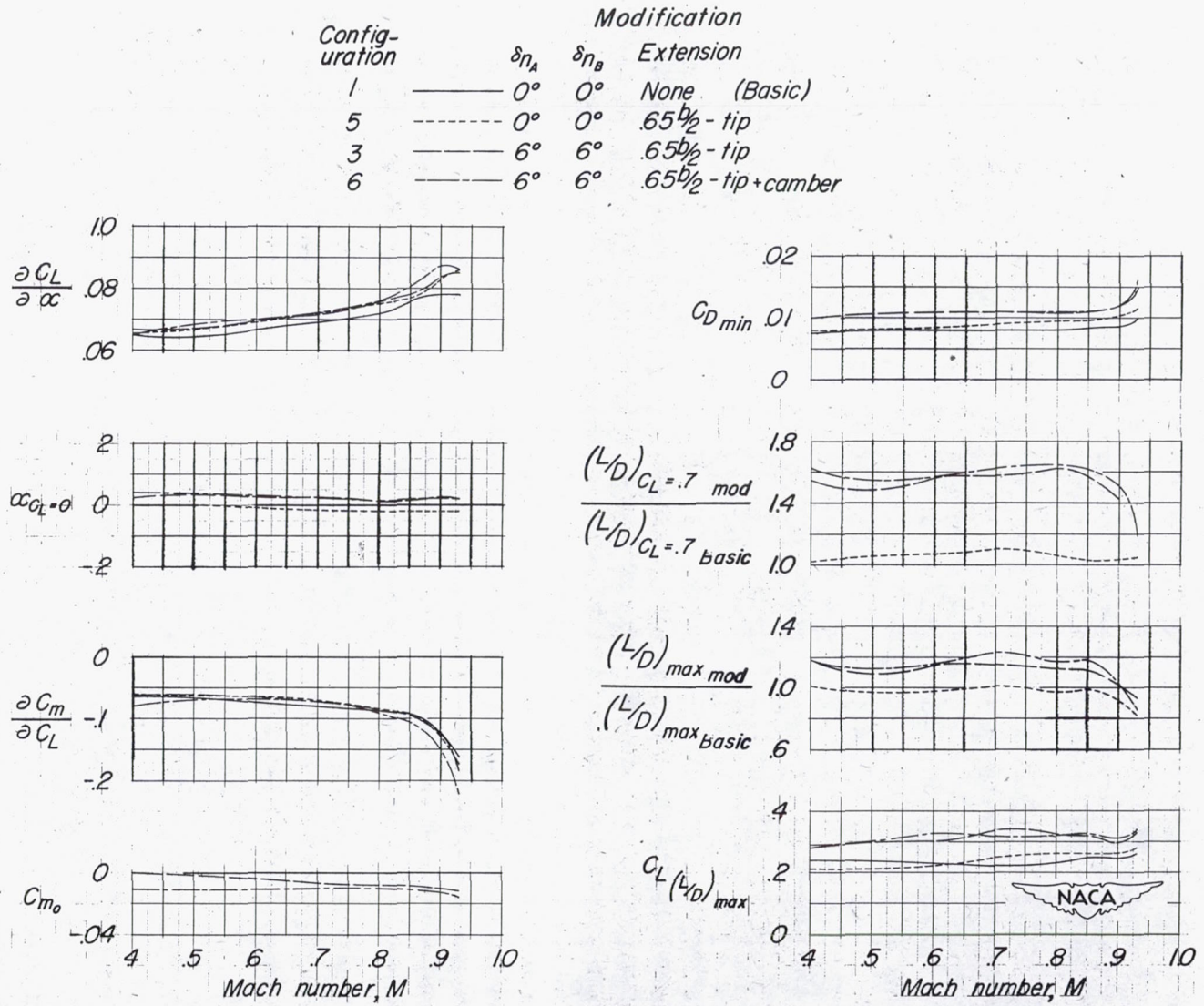

Figure 16.- Summary of aerodynamic characteristics of wing-fuselage combination showing effects of $0.10\bar{c}$ chord-extension alone and $0.10\bar{c}$ chord-extension with camber added to leading edge.

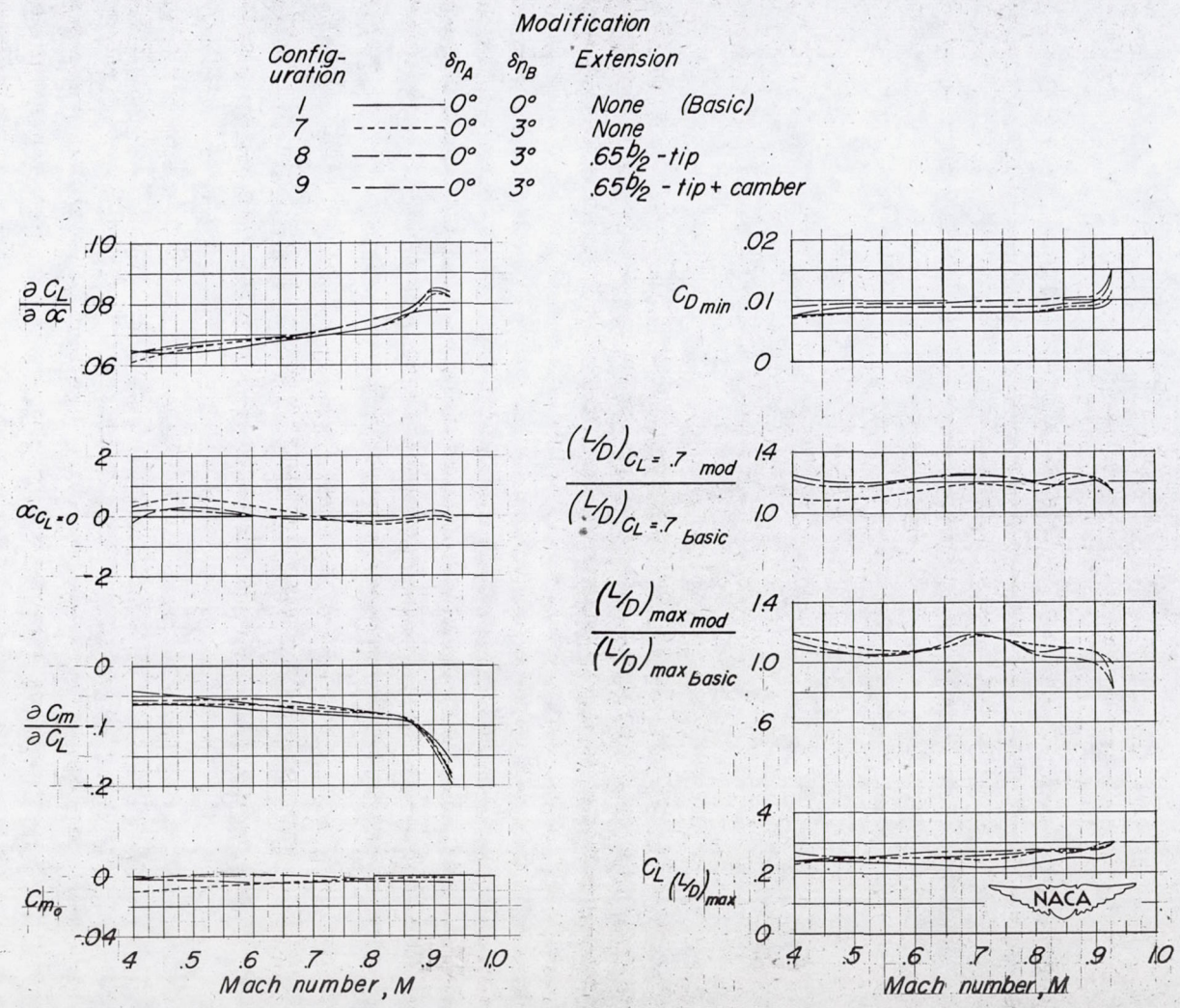

Figure 17.- Summary of aerodynamic characteristics of wing-fuselage combination showing effects of partial-span leading-edge flaps, 0.10$\bar{c}$ chord-extension, and 0.10$\bar{c}$ chord-extension with camber added to leading edge.

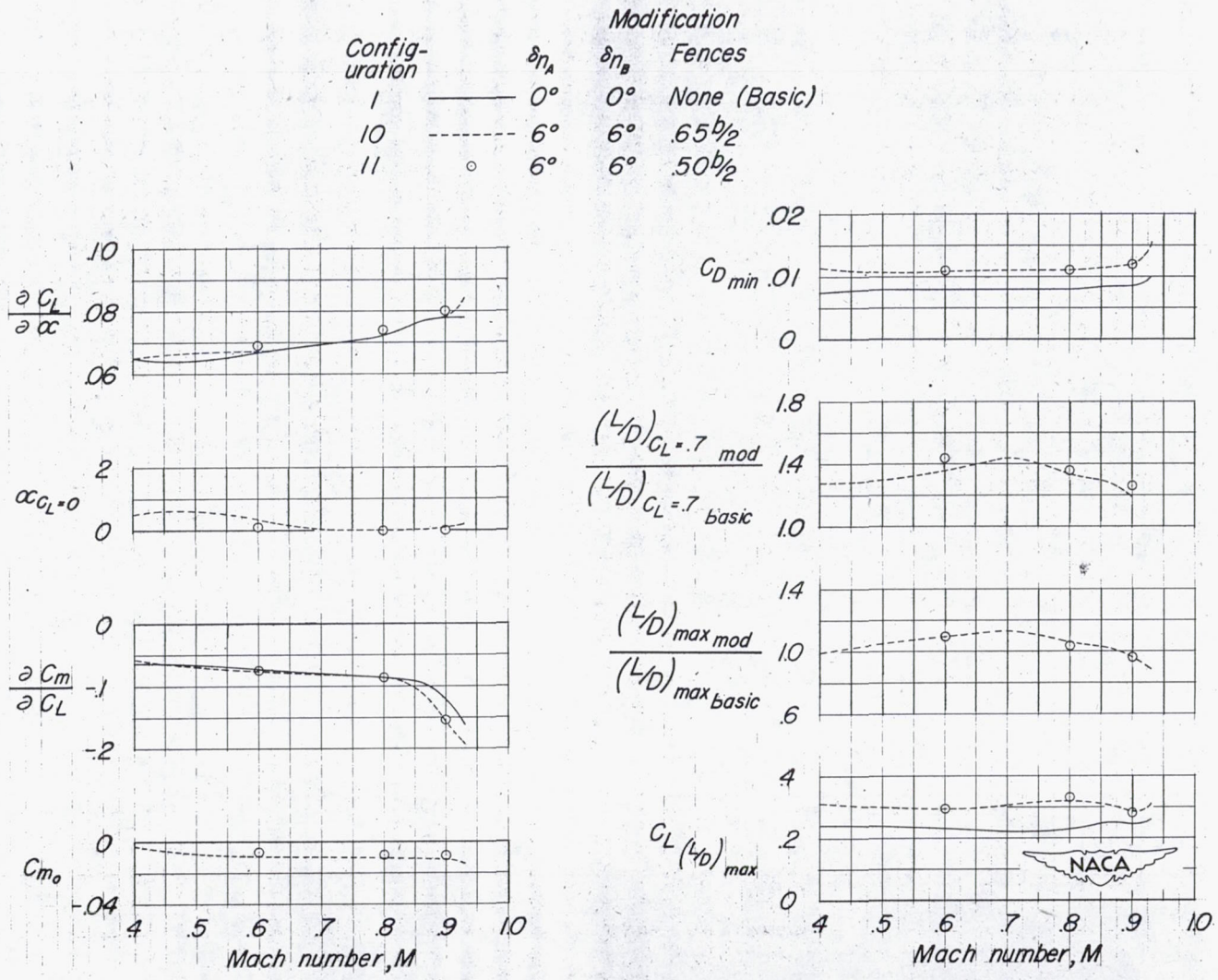

Figure 18.- Summary of aerodynamic characteristics of wing-fuselage combination showing effects of fences in combination with full-span leading-edge flaps.